

Robust Transmission Design for RIS-assisted Secure Multiuser Communication Systems in the Presence of Hardware Impairments

Zhangjie Peng, Ruisong Weng, Cunhua Pan, *Member, IEEE*, Gui Zhou, *Student Member, IEEE*, Marco Di Renzo, *Fellow, IEEE*, and A. Lee Swindlehurst, *Fellow, IEEE*

Abstract—This paper investigates reconfigurable intelligent surface (RIS)-assisted secure multiuser communication systems subject to hardware impairments (HIs). We jointly optimize the beamforming vectors at the base station (BS) and the phase shifts of the reflecting elements at the RIS so as to maximize the weighted minimum secrecy rate (WMSR), subject to both transmission power constraints at the BS and unit-modulus constraints at the RIS. To address the formulated optimization problem, we first decouple it into two tractable subproblems and then use the block coordinate descent (BCD) method to alternately optimize the subproblems. Two different methods are proposed to solve the two obtained subproblems. The first method transforms each subproblem into a second order cone programming (SOCP) problem, which can be directly solved using CVX. The second method leverages the Minorization-Maximization (MM) algorithm. Specifically, we first derive a concave approximation function, which is a lower bound of the original objective function, and then the two subproblems are transformed into two simple surrogate problems with closed-form solutions. Simulation results verify the performance gains of the proposed robust transmission method over existing non-robust designs. In addition, the MM algorithm is shown to have much lower complexity than the SOCP-based algorithm.

Index Terms—Intelligent reflecting surface (IRS), reconfigurable intelligent surface (RIS), hardware impairments (HIs), physical layer security (PLS).

I. INTRODUCTION

Thanks to the growing popularization of mobile devices, the global wireless network capacity is expected to increase 100-fold by 2030 [1]. Furthermore, emerging applications, such as the industrial Internet of things, virtual reality (VR) and augmented reality (AR) [2], have high quality of service (QoS) requirements, such as ultra-low latency, ultra-high reliability and extremely high data rates [3]. Some potential techniques, such as massive multiple-input multiple-output (m-MIMO) arrays, millimeter wave (mmWave) and terahertz (THz) communications [4], have been proposed to meet the above

requirements. However, these technologies usually result in increasing the cost of network deployment and the network power consumption [5].

Another emerging technology for fulfilling the high QoS requirements of future networks [6], [7] is the use of reconfigurable intelligent surfaces (RISs). RIS is a thin metamaterial layer that is composed of an array of low cost reflecting elements integrated with low power and controllable electronics [8]. Due to the absence of power amplifiers, digital signal processing units, and multiple radio frequency chains, the main features of an RIS include a low implementation cost, a low power consumption, and an easy deployment, as well as the capability of reconfiguring the wireless environment [9], [10]. Broadly speaking, an RIS is a dynamic metasurface whose electromagnetic characteristics can be dynamically adjusted through control signals. For example, the electromagnetic waves that impinge upon an RIS can be steered towards different directions, by simply optimizing the phase response of each of its constituent scattering elements [11]. An RIS can be utilized to enhance the desired signal power, to mitigate the network interference, and to reduce the electromagnetic pollution since no additional signals are generated [12]. Compared with traditional active antenna arrays that are equipped with multiple active radio frequency transceivers, an RIS reradiates the incident signals by simply adjusting the amplitude and the phase shift of the reflecting elements, which can be realized by controlling the junction voltage of PIN diodes or varactors [13]. RISs can be deployed on, e.g., the facades of buildings, the interior walls of offices, and windows.

RISs can be utilized for enhancing the security of wireless networks and have been recently amalgamated with physical layer security (PLS) [14], [15]. Traditional wireless security methods encrypt the data at the network layer. This usually requires a high overhead due to the frequent distribution and management of secrecy keys [16]–[18]. PLS is an alternative solution that makes use of the properties of the wireless communication medium and the transceiver hardware to enable critical aspects of secure communications. However, conventional PLS techniques only focus on beamforming design at the transceivers, and may not provide good performance in some scenarios, e.g., when the legitimate user and the eavesdropper have highly correlated channels (e.g., when they are located in the same direction from the transmitter) [19]. Thanks to the capability of reconfiguring the propagation environment as desired, RISs have several applications in the context of PLS for improving the security of wireless

Z. Peng, and R. Weng are with the College of Information, Mechanical and Electrical Engineering, Shanghai Normal University, Shanghai 200234, China (e-mails: pengzhangjie@shnu.edu.cn, 1000497102@smail.shnu.edu.cn).

C. Pan is with the National Mobile Communications Research Laboratory, Southeast University, China. (cunhuapan21@gmail.com).

G. Zhou is with the School of Electronic Engineering and Computer Science at Queen Mary University of London, London E1 4NS, U.K. (email: g.zhou@qmul.ac.uk).

M. Di Renzo is with Université Paris-Saclay, CNRS, CentraleSupélec, Laboratoire des Signaux et Systèmes, 91192 Gif-sur-Yvette, France (e-mail: marco.di-renzo@universite-paris-saclay.fr).

A. L. Swindlehurst is with the Department of Electrical Engineering and Computer Science, University of California at Irvine, Irvine, CA 92697 USA (e-mail: swindle@uci.edu).

communication systems [20]–[23]. For example, the authors of [20] studied the secrecy outage probability of an RIS-assisted single-antenna system where only one eavesdropper exist. In [21], the authors proposed a robust algorithm to maximize the achievable secrecy rate of a multi-user multiple-input single-output (MISO) system. In [22], the authors proposed a deep reinforcement learning (DRL)-based scheme to improve the security performance of RIS-assisted MIMO systems. The authors of [23] analyzed the security performance gains when deploying an RIS in unmanned aerial vehicle (UAV)-assisted mmWave wireless communication networks.

The existing contributions on RIS-assisted PLS assume that the transceivers are constructed with ideal and perfect hardware components. In practical communication systems, low-cost hardware is often preferred even though such hardware may be subject to hardware impairments (HIs) such as I/Q-imbalance, amplifier non-linearities, quantization errors, and phase noise [24]. If these hardware impairments are ignored at the design stage, the performance usually degrades [25]. Recently, the impact of HIs on the security performance of RIS-assisted single-user systems has been analyzed [26], [27]. Specifically, the authors of [26] proposed a robust algorithm to maximize the secrecy rate in the presence of HIs. In [27], the authors derived an approximate closed-form expression for the secrecy outage probability and studied the impact of HIs on the system performance.

In this paper, we investigate the security performance of RIS-assisted multiuser MISO systems in the presence of HIs. Unlike the single-user scenarios considered in [26] and [27], we assume a scenario with multiple legitimate users whose information security is threatened by an eavesdropper. By deploying an RIS, we aim to improve the security performance under the premise of ensuring fairness among the users. However, due to the considered complex scenario, the resulting optimization problem cannot be directly solved by using existing methods. Thus, we propose tractable algorithms to tackle the formulated optimization problem. Specifically, the main contributions of this paper are summarized as follows:

- 1) This work is the first to consider RIS-aided secure communications in multiuser MISO systems, where both the base station (BS) and the legitimate users are subject to HIs. By optimizing the BS precoding matrix and the RIS reflection coefficients, we formulate a fairness-based joint optimization problem that maximizes the weighted minimum secrecy rate (WMSR), subject to both transmission power and unit modulus constraints.
- 2) To efficiently solve the non-convex problem, we propose a benchmark algorithm based on the block coordinate descent (BCD) method. Specifically, we first decouple the original problem into multiple tractable subproblems by invoking the semidefinite relaxation (SDR) and the weighted minimum mean-square error (WMMSE) criterion. The precoding and the reflection coefficient subproblems are transformed into second order cone programming (SOCP) problems. Then, these two subproblems are alternately solved until convergence.
- 3) Also, we propose a minorization-maximization (MM) algorithm to reduce the computational complexity. In

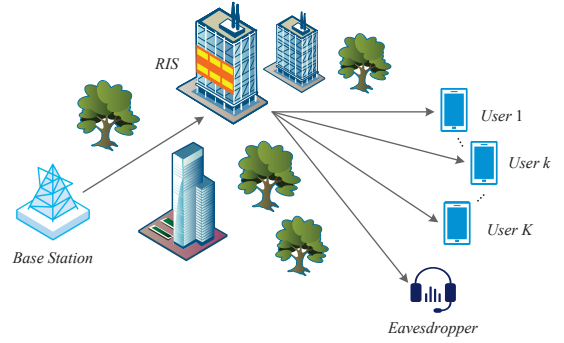


Fig. 1. An RIS-assisted MISO downlink system with an N -antenna BS, a single-antenna eavesdropper and K single-antenna users.

particular, we first derive a concave smooth function as a lower bound of the original non-differentiable objective function. Then, we apply the MM algorithm to obtain a surrogate function which has a closed-form solution.

- 4) Finally, we present simulation results to verify the effectiveness of the proposed schemes and the advantages of the proposed robust transmission design for secure communications. We demonstrate that deploying an RIS can effectively improve the security performance of multiuser wireless communication systems in the presence of HIs. The convergence and effectiveness of the proposed algorithm are verified as well.

The rest of this paper is organized as follows. Section II introduces the RIS-assisted wireless communication system model subject to HIs and formulates the WMSR problem. Section III decouples the original problem into multiple tractable sub-problems and proposes a benchmark optimization algorithm based on the BCD method. In Section IV, a low-complexity MM algorithm is introduced. Simulation results are given in Section V and Section VI concludes this paper.

Notation: Constants, column vectors and matrices are denoted by italics, boldface lowercase letters and boldface uppercase letters, respectively. $\text{Re}\{b\}$, $|b|$ and $\angle(b)$ denote the real part, modulus and angle of the complex number b , respectively. $\|\mathbf{b}\|_1$ and $\|\mathbf{b}\|_2$ denote the 1-norm and 2-norm of vector \mathbf{b} , respectively. $\text{diag}(\cdot)$ and $\text{vec}(\cdot)$ represent the diagonalization and vectorization operators, respectively. \mathbf{B}^T , \mathbf{B}^* , \mathbf{B}^H , $\text{Tr}[\mathbf{B}]$ and $\|\mathbf{B}\|_F$ denote the transpose, conjugate, Hermitian, trace and Frobenius norm of matrix \mathbf{B} , respectively. The Hadamard product and Kronecker product of two matrices \mathbf{B} and \mathbf{C} are expressed as $\mathbf{B} \odot \mathbf{C}$ and $\mathbf{B} \otimes \mathbf{C}$, respectively. $\mathbf{B} \succeq \mathbf{C}$ indicates that $\mathbf{B} - \mathbf{C}$ is a positive semidefinite matrix. \mathbb{C} denotes the complex field and $j \triangleq \sqrt{-1}$ is the imaginary unit.

II. SYSTEM MODEL

A. Signal Transmission Model

We consider an RIS-assisted MISO downlink system with a BS, an eavesdropper and K legitimate users, as illustrated in Figure 1. The BS is equipped with $N > 1$ transmit antennas to serve the legitimate users in the presence of the eavesdropper. In practice, the direct communication links may be blocked by various obstacles, such as tall outdoor buildings. In this case, an RIS consisting of M reflecting elements is

deployed to ensure the secure transmission of data. The set of RIS reflection coefficients is collected in the diagonal matrix $\Phi = \text{diag}(\phi)$, where $\phi = [\phi_1, \dots, \phi_M]^T$ with $|\phi_m|^2 = 1$, $\forall m = 1, \dots, M$. The baseband channels between the BS and the RIS, the RIS and the legitimate user k , and the RIS and the eavesdropper are denoted by $\mathbf{H}_{\text{BI}} \in \mathbb{C}^{M \times N}$, $\mathbf{h}_{\text{I},k} \in \mathbb{C}^{M \times 1}$, $\mathbf{g}_{\text{I}} \in \mathbb{C}^{M \times 1}$, respectively.

The signal transmitted from the BS is modeled as

$$\mathbf{x} = \hat{\mathbf{x}} + \boldsymbol{\eta}_t, \quad (1)$$

$$\hat{\mathbf{x}} \triangleq \sum_{k=1}^K \mathbf{w}_k s_k, \quad (2)$$

where s_k is assumed to be an independent random Gaussian signal with zero mean and variance $\mathbb{E}[|s_k|^2] = 1$. In addition, $\mathbf{w}_k \in \mathbb{C}^{N \times 1}$ is the corresponding beamforming vector. Hence, the precoding matrix of the BS can be defined as $\mathbf{W} \triangleq [\mathbf{w}_1, \dots, \mathbf{w}_K] \in \mathbb{C}^{N \times K}$, which satisfies the constraint $\text{Tr}(\mathbf{W}^H \mathbf{W}) \leq P$, where P represents the maximum transmit power.

The additional distortion noise term $\boldsymbol{\eta}_t$ describes the impact of HIs at the transmitter. According to the model in [28], [29], the distortion noise is assumed to be proportional to the signal power. In particular, the entries of $\boldsymbol{\eta}_t$ are independent zero-mean Gaussian random variables whose distribution is $\mathcal{CN}(0, \Upsilon_t)$, where $\Upsilon_t = \kappa_t \text{diag}(\mathbf{W} \mathbf{W}^H)$ and $\kappa_t \geq 0$ is the ratio between the transmit distorted noise power and the transmit signal power.

The signal received at user k is given by

$$\begin{aligned} y_{\text{U},k} &= (\mathbf{h}_{\text{I},k}^H \Phi \mathbf{H}_{\text{BI}}) \mathbf{x} + \eta_{\text{r},k} + n_{\text{U},k} \\ &\triangleq \hat{y}_{\text{U},k} + \eta_{\text{r},k}, \end{aligned} \quad (3)$$

where $n_{\text{U},k}$ is the additive white Gaussian noise (AWGN) whose distribution is $\mathcal{CN}(0, \delta_{\text{U},k}^2)$. $\eta_{\text{r},k}$ is an additional distortion noise term that is independent of $\hat{y}_{\text{U},k}$ and whose distribution is $\mathcal{CN}(0, \gamma_{\text{r},k})$, with $\gamma_{\text{r},k}$ being defined as $\gamma_{\text{r},k} = \mathbb{E}\{\kappa_{\text{r},k} |\hat{y}_{\text{U},k}|^2\} = \kappa_{\text{r},k} \mathbf{h}_{\text{U},k}^H (\mathbf{W} \mathbf{W}^H + \kappa_t \text{diag}(\mathbf{W} \mathbf{W}^H)) \mathbf{h}_{\text{U},k}$, where $\kappa_{\text{r},k} \geq 0$ is the ratio between the distorted noise power and the undistorted received signal power [26]. The achievable rate of user k is given by

$$R_{\text{U},k} = \log \left(1 + \frac{|\mathbf{h}_{\text{U},k}^H \mathbf{w}_k|^2}{\sum_{\substack{i=1 \\ i \neq k}}^K |\mathbf{h}_{\text{U},k}^H \mathbf{w}_i|^2 + \mathbf{h}_{\text{U},k}^H \Upsilon_t \mathbf{h}_{\text{U},k} + \gamma_{\text{r},k} + \delta_{\text{U},k}^2} \right), \quad (4)$$

where

$$\begin{aligned} e_{\text{U},k} &= \mathbb{E} \left[(\hat{s}_{\text{U},k} - s_k)^H (\hat{s}_{\text{U},k} - s_k) \right] \\ &= \mathbb{E} \left[u_{\text{U},k}^* u_{\text{U},k} \left((1 + \kappa_{\text{r},k}) \mathbf{h}_{\text{U},k}^H \left(\sum_{k=1}^K (\mathbf{w}_k s_k s_k^* \mathbf{w}_k^H) + \Upsilon_t \right) \mathbf{h}_{\text{U},k} + \delta_{\text{U},k}^2 \right) + s_k s_k^* - 2 \text{Re} \{ u_{\text{U},k}^* \mathbf{h}_{\text{U},k}^H \mathbf{w}_k s_k s_k^* \} \right] \\ &= u_{\text{U},k}^* u_{\text{U},k} (1 + \kappa_{\text{r},k}) \mathbf{h}_{\text{U},k}^H (\mathbf{W} \mathbf{W}^H + \kappa_t \text{diag}(\mathbf{W} \mathbf{W}^H)) \mathbf{h}_{\text{U},k} + u_{\text{U},k}^* u_{\text{U},k} \delta_{\text{U},k}^2 + 1 - 2 \text{Re} \{ u_{\text{U},k}^* \mathbf{h}_{\text{U},k}^H \mathbf{W} \mathbf{t}_k \}. \end{aligned} \quad (16)$$

$$\mathbf{h}_{\text{U},k}^H \triangleq \mathbf{h}_{\text{I},k}^H \Phi \mathbf{H}_{\text{BI}}. \quad (5)$$

We consider the worst-case assumption that the eavesdropper can eliminate most of the noise with the exception of the distortion noise of the transmitter hardware. Also, we assume that it can decode and cancel the interference from other users [30]. Therefore, the signal received at the eavesdropper is given by

$$y_{\text{E}} = (\mathbf{g}_{\text{I}}^H \Phi \mathbf{H}_{\text{BI}}) \mathbf{x} + n_{\text{E}}, \quad (6)$$

where n_{E} is AWGN whose distribution is $\mathcal{CN}(0, \delta_{\text{E}}^2)$ and the achievable rate of the eavesdropper associated with user k is

$$R_{\text{E},k} = \log \left(1 + \frac{|\mathbf{h}_{\text{E}}^H \mathbf{w}_k|^2}{\mathbf{h}_{\text{E}}^H \Upsilon_t \mathbf{h}_{\text{E}} + \delta_{\text{E}}^2} \right), \quad (7)$$

where

$$\mathbf{h}_{\text{E}}^H \triangleq \mathbf{g}_{\text{I}}^H \Phi \mathbf{H}_{\text{BI}}. \quad (8)$$

Accordingly, the secrecy rate R_k of the legitimate user k in nats/second/Hertz (nat/s/Hz) is given by

$$R_k \triangleq [R_{\text{U},k} - R_{\text{E},k}]^+, \quad (9)$$

where $[a]^+ \triangleq \max(a, 0)$.

B. Problem Formulation

To maximize the WMSR while ensuring fairness, we consider the joint optimization of the precoding matrix \mathbf{W} and the reflection coefficient vector ϕ . By denoting the weighting factor of user k by ω_k , the WMSR problem is formulated as

$$\max_{\mathbf{W}, \phi} \min_{k \in \mathcal{K}} \{ \omega_k R_k \} \quad (10a)$$

$$\text{s.t. } \text{Tr}(\mathbf{W}^H \mathbf{W}) \leq P, \quad (10b)$$

$$\phi \in \mathcal{S}, \quad (10c)$$

where the set $\mathcal{S} \triangleq \{\phi \mid |\phi_m| = 1, 1 \leq m \leq M\}$ imposes the unit-modulus constraint on ϕ and $\mathcal{K} \triangleq \{1, 2, \dots, K\}$. Compared to a system model with no HIs, the objective function of the problem in (10) is more complex. The analysis of the secrecy rate instead of the information rate further complicates the objective to the point that a direct solution becomes intractable. To circumvent these issues, we propose two efficient algorithms in the next sections.

III. BCD-SOCP ALGORITHM

In this section, we propose a BCD-SOCP algorithm to solve the WMSR problem in (10). Specifically, we first decouple the problem in (10) into two subproblems, each of which is converted into an SOCP problem that can be efficiently solved. The two subproblems are then alternately solved until convergence.

A. Problem Reformulation

To tackle the complexity of the objective function in (10), we write R_k as the sum of three parts, i.e.,

$$\begin{aligned} R_k(\mathbf{W}, \phi) &= R_{U,k}(\mathbf{W}, \phi) - R_{E,k}(\mathbf{W}, \phi) \\ &= R_{U,k}(\mathbf{W}, \phi) - \log \left(\frac{|\mathbf{h}_E^H \mathbf{w}_k|^2 + \mathbf{h}_E^H \Upsilon_t \mathbf{h}_E + \delta_E^2}{\mathbf{h}_E^H \Upsilon_t \mathbf{h}_E + \delta_E^2} \right) \\ &= f_{1,k}(\mathbf{W}, \phi) + f_{2,k}(\mathbf{W}, \phi) + f_3(\mathbf{W}, \phi), \end{aligned} \quad (11)$$

where

$$f_{1,k}(\mathbf{W}, \phi) \triangleq R_{U,k}(\mathbf{W}, \phi) \quad (12)$$

$$f_{2,k}(\mathbf{W}, \phi) \triangleq -\log \left(1 + \frac{|\mathbf{h}_E^H \mathbf{w}_k|^2 + \mathbf{h}_E^H \Upsilon_t \mathbf{h}_E}{\delta_E^2} \right) \quad (13)$$

$$f_3(\mathbf{W}, \phi) \triangleq \log \left(1 + \frac{\mathbf{h}_E^H \Upsilon_t \mathbf{h}_E}{\delta_E^2} \right). \quad (14)$$

In the following, we derive lower bounds for $f_{1,k}$, $f_{2,k}$ and f_3 .

As far as $f_{1,k}$ is concerned, we derive a lower bound by exploiting the equivalence between the data rate and the WMMSE [31]. By denoting the decoding variable of the legitimate user k as $u_{U,k}$, the corresponding estimated symbol can be written as

$$\hat{s}_{U,k} = u_{U,k}^* y_{U,k}. \quad (15)$$

Denote the set of decoding variables as $\mathcal{U} = \{u_{U,k}, k \in \mathcal{K}\}$. According to (15), the mean squared error (MSE) of $\hat{s}_{U,k}$ is equal to $e_{U,k}$ given in (16) at the bottom of this page, where $\mathbf{t}_k \in \mathbb{C}^{K \times 1}$ is a vector whose single non-zero element is “1” at the k -th position. According to [32], by introducing a set of auxiliary variables $\mathcal{V} = \{v_k \geq 0, k \in \mathcal{K}\}$, a lower bound for $f_{1,k}$ can be expressed as

$$\tilde{f}_{1,k}(\mathbf{W}, \phi, \mathcal{U}, \mathcal{V}) = \log |v_k| - v_k e_{U,k} + 1. \quad (17)$$

The relationship between $f_{1,k}$ and $\tilde{f}_{1,k}$ is

$$f_{1,k}(\mathbf{W}, \phi) = \max_{\mathcal{U}, \mathcal{V}} \tilde{f}_{1,k}(\mathbf{W}, \phi, \mathcal{U}, \mathcal{V}), \quad (18)$$

where the optimal solutions for $u_{U,k}$ and v_k can be formulated as

$$u_{U,k}^{\text{opt}} = \frac{\mathbf{h}_{U,k}^H \mathbf{w}_k}{\sum_{i=1}^K |\mathbf{h}_{U,k}^H \mathbf{w}_i|^2 + \mathbf{h}_{U,k}^H \Upsilon_t \mathbf{h}_{U,k} + \gamma_{r,k} + \delta_{U,k}^2}, \quad (19)$$

$$v_k^{\text{opt}} = e_{U,k}^{-1}. \quad (20)$$

As far as $f_{2,k}$ is concerned, we introduce the following lemma to obtain a lower bound.

Lemma 1 [33]: Consider the function $f(\bar{y}) = -\bar{y}\bar{x} + \log \bar{y} + 1$ for any $\bar{x} > 0$. Then, we have

$$-\log \bar{x} = \max_{\bar{y} > 0} f(\bar{y}), \quad (21)$$

and the optimal solution is $\bar{y} = \frac{1}{\bar{x}}$. ■

The lemma shows that $f(\bar{y})$ is a lower bound of $-\log \bar{x}$, and this bound is tight when $\bar{y} = \frac{1}{\bar{x}}$. Let us denote $\mathcal{D} = \{d_k \geq 0, k \in \mathcal{K}\}$ and define $\bar{x} = 1 + \frac{|\mathbf{h}_E^H \mathbf{w}_k|^2 + \mathbf{h}_E^H \Upsilon_t \mathbf{h}_E}{\delta_E^2}$, $\bar{y} = d_k$. Then, a lower bound for $f_{2,k}$ is given by $\tilde{f}_{2,k}$ defined as

$$f_{2,k}(\mathbf{W}, \phi) = \max_{d_k} \tilde{f}_{2,k}(\mathbf{W}, \phi, \mathcal{D}), \quad (22)$$

where

$$\begin{aligned} \tilde{f}_{2,k}(\mathbf{W}, \phi, \mathcal{D}) &= -d_k \left(1 + \frac{|\mathbf{h}_E^H \mathbf{w}_k|^2 + \mathbf{h}_E^H \Upsilon_t \mathbf{h}_E}{\delta_E^2} \right) \\ &\quad + \log d_k + 1, \end{aligned} \quad (23)$$

and the optimal solution for d_k is

$$d_k^{\text{opt}} = \left(1 + \frac{|\mathbf{h}_E^H \mathbf{w}_k|^2 + \mathbf{h}_E^H \Upsilon_t \mathbf{h}_E}{\delta_E^2} \right)^{-1}. \quad (24)$$

Finally, to find a lower bound for f_3 that is given in a tractable analytical form, we utilize the following lemma.

Lemma 2 [34]: Given the complex vector $\bar{\mathbf{y}}$, the function $f(\bar{\mathbf{y}}, \bar{\mathbf{x}}) = (|\bar{\mathbf{x}}|^2 + \delta^2) |\bar{\mathbf{y}}|^2 - 2\text{Re} \{ \bar{\mathbf{y}}^H \bar{\mathbf{x}} \} + 1$ satisfies

$$\frac{\delta^2}{|\bar{\mathbf{x}}|^2 + \delta^2} = \min_{\bar{\mathbf{y}}} f(\bar{\mathbf{y}}, \bar{\mathbf{x}}), \quad (25)$$

and the optimal solution is $\bar{\mathbf{y}} = \frac{\bar{\mathbf{x}}}{|\bar{\mathbf{x}}|^2 + \delta^2}$. ■

The lemma provides an upper bound for $\frac{\delta^2}{|\bar{\mathbf{x}}|^2 + \delta^2}$, which is tight when $\bar{\mathbf{y}} = \frac{\bar{\mathbf{x}}}{|\bar{\mathbf{x}}|^2 + \delta^2}$. Then, let us introduce a new variable $\tilde{\mathbf{w}} = \text{vec}(\mathbf{W})$. Due to the complexity of f_3 , we derive the corresponding lower bounds for the following two cases: 1) Case A: Given the other variables, $\tilde{\mathbf{w}}$ is the only variable to be optimized; 2) Case B: Given the other variables, ϕ is the only variable to be optimized.

1) *Case A: Given the other variables, $\tilde{\mathbf{w}}$ is the only variable to be optimized.* Based on Lemma 1 and Lemma 2, a lower bound for $f_3(\tilde{\mathbf{w}})$ can be obtained as stated in the following lemma.

Lemma 3: Let us introduce the auxiliary variables p_w and \mathbf{q}_w . A lower bound for $f_3(\tilde{\mathbf{w}})$ is given by

$$\tilde{f}_{3,\tilde{\mathbf{w}}}(\tilde{\mathbf{w}}) = -\tilde{\mathbf{w}}^H \tilde{\mathbf{C}}_{3,w} \tilde{\mathbf{w}} + 2\text{Re} \{ \tilde{\mathbf{b}}_{3,w}^H \tilde{\mathbf{w}} \} + \tilde{c}_{3,w}, \quad (26)$$

where

$$\tilde{\mathbf{C}}_{3,w} \triangleq p_w |\mathbf{q}_w|^2 \mathbf{L}^T \mathbf{L}, \quad (27a)$$

$$\tilde{\mathbf{b}}_{3,w} \triangleq \mathbf{L}^T \mathbf{q}_w, \quad (27b)$$

$$\tilde{c}_{3,w} \triangleq -p_w |\mathbf{q}_w|^2 \delta_E^2 - p_w + \log p_w + 1, \quad (27c)$$

$$\mathbf{L}^T \mathbf{L} \triangleq (\mathbf{I}_K \otimes \text{diag}(\mathbf{h}_E \mathbf{h}_E^H)), \quad (27d)$$

and \mathbf{I}_K denotes the $K \times K$ identity matrix. Additionally, the optimal solutions for p_w and \mathbf{q}_w are given by

$$p_w^{\text{opt}} = \left(1 + \frac{\mathbf{h}_E^H \Upsilon_t \mathbf{h}_E}{\delta_E^2} \right), \quad (28)$$

$$\mathbf{q}_w^{\text{opt}} = \frac{\mathbf{L} \tilde{\mathbf{w}}}{|\mathbf{L} \tilde{\mathbf{w}}|^2 + \delta_E^2}. \quad (29)$$

Proof: See Appendix A. ■

2) *Case B: Given the other variables, ϕ is the only variable to be optimized.* Based on Lemma 1 and Lemma 2, a lower bound for $f_3(\phi)$ can be obtained as stated in the following lemma.

Lemma 4: Let us introduce the auxiliary variables p_ϕ and \mathbf{q}_ϕ . A lower bound for $f_3(\phi)$ is given by

$$\tilde{f}_{3,\phi}(\phi) = -\phi^H \tilde{\mathbf{C}}_{3,\phi} \phi + 2\text{Re} \{ \tilde{\mathbf{b}}_{3,\phi}^H \phi \} + \tilde{c}_{3,\phi}, \quad (30)$$

where

$$\tilde{\mathbf{C}}_{3,\phi} \triangleq p_\phi |\mathbf{q}_\phi|^2 \left((\mathbf{g}_I \mathbf{g}_I^H) \odot (\mathbf{H}_{\text{BI}} \mathbf{J}^T \mathbf{J} \mathbf{H}_{\text{BI}}^H)^T \right), \quad (31a)$$

$$\tilde{\mathbf{b}}_{3,\phi} \triangleq \left[[p_\phi \mathbf{H}_{\text{BI}} \mathbf{J}^T \mathbf{q}_\phi \mathbf{g}_I^H]_{1,1}, \dots, [p_\phi \mathbf{H}_{\text{BI}} \mathbf{J}^T \mathbf{q}_\phi \mathbf{g}_I^H]_{M,M} \right]^T, \quad (31b)$$

$$\tilde{c}_{3,\phi} \triangleq -p_\phi |\mathbf{q}_\phi|^2 \delta_E^2 - p_\phi + \log p_\phi + 1, \quad (31c)$$

$$\mathbf{J}^T \mathbf{J} \triangleq \text{diag}(\mathbf{W} \mathbf{W}^H). \quad (31d)$$

Additionally, the optimal solutions for p_ϕ and \mathbf{q}_ϕ are given by

$$p_\phi^{\text{opt}} = \left(1 + \frac{\mathbf{h}_E^H \boldsymbol{\Upsilon}_t \mathbf{h}_E}{\delta_E^2} \right), \quad (32)$$

$$\mathbf{q}_\phi^{\text{opt}} = \frac{\mathbf{J} \mathbf{h}_E}{|\mathbf{h}_E^H \mathbf{J}^T|^2 + \delta_E^2}. \quad (33)$$

Proof: See Appendix B. ■

Thus, by denoting $\mathcal{P} = \{p_w, p_\phi\}$, $\mathcal{Q} = \{\mathbf{q}_w, \mathbf{q}_\phi\}$, a lower bound for f_3 is expressed as

$$\tilde{f}_3(\tilde{\mathbf{w}}, \phi, \mathcal{P}, \mathcal{Q}) \triangleq \begin{cases} \tilde{f}_{3,\tilde{\mathbf{w}}}(\tilde{\mathbf{w}}, \phi, \mathcal{P}, \mathcal{Q}), & \text{Case A} \\ \tilde{f}_{3,\phi}(\tilde{\mathbf{w}}, \phi, \mathcal{P}, \mathcal{Q}), & \text{Case B} \end{cases}. \quad (34)$$

Finally, from (11), (17), (22) and (34), a lower bound for R_k can be expressed as

$$\tilde{R}_k = \left[\tilde{f}_{1,k}(\tilde{\mathbf{w}}, \phi, \mathcal{U}, \mathcal{V}) + \tilde{f}_{2,k}(\tilde{\mathbf{w}}, \phi, \mathcal{D}) + \tilde{f}_3(\tilde{\mathbf{w}}, \phi, \mathcal{P}, \mathcal{Q}) \right]^+, \quad (35)$$

and the problem in (10) can be reformulated as

$$\max_{\tilde{\mathbf{w}}, \phi, \mathcal{U}, \mathcal{V}, \mathcal{D}, \mathcal{P}, \mathcal{Q}} \min_{k \in \mathcal{K}} \left\{ \omega_k \tilde{R}_k \right\} \quad (36a)$$

$$\text{s.t. } \tilde{\mathbf{w}}^H \tilde{\mathbf{w}} \leq P, \quad (36b)$$

$$\phi \in \mathcal{S}. \quad (36c)$$

To solve the problem in (36), we use the BCD method to alternately optimize each variable in the objective function, while keeping the other variables fixed. The optimal solutions for \mathcal{U} , \mathcal{V} , \mathcal{D} , \mathcal{P} and \mathcal{Q} are given in (19), (20), (24), (28), (32), (29), and (33), respectively. On the other hand, the optimization of the precoding vector $\tilde{\mathbf{w}}$ and the reflection coefficient vector ϕ is addressed in the following sections.

B. Optimization of the Precoding Vector $\tilde{\mathbf{w}}$

In this subsection, $\tilde{\mathbf{w}}$ is optimized under the assumption that all the other variables are kept fixed. Since the lower bound $\tilde{f}_{3,\tilde{\mathbf{w}}}$ in (26) is a quadratic function in the optimization variable, we rewrite $\tilde{f}_{1,k}(\tilde{\mathbf{w}})$ and $\tilde{f}_{2,k}(\tilde{\mathbf{w}})$ as quadratic functions as well.

1) *Mathematical Derivation of $\tilde{f}_{1,k}(\tilde{\mathbf{w}})$.* $\tilde{f}_{1,k}(\tilde{\mathbf{w}})$ in (17) can be reformulated as

$$\begin{aligned} \tilde{f}_{1,k}(\tilde{\mathbf{w}}) &= 2\text{Re} \left\{ v_k u_{\text{U},k}^* \mathbf{h}_{\text{U},k}^H \mathbf{W} \mathbf{t}_k \right\} - v_k u_{\text{U},k}^* u_{\text{U},k} \\ &\quad \times \left((1 + \kappa_{\text{r},k}) \text{Tr} \left[\mathbf{W}^H (\mathbf{h}_{\text{U},k} \mathbf{h}_{\text{U},k}^H + \kappa_t \text{diag}(\mathbf{h}_{\text{U},k} \mathbf{h}_{\text{U},k}^H)) \mathbf{W} \right] \right) \\ &\quad + \log |v_k| - v_k u_{\text{U},k}^* u_{\text{U},k} \delta_{\text{U},k}^2 - v_k + 1 \\ &= 2\text{Re} \left\{ \text{Tr} [\mathbf{B}_{1,w,k} \mathbf{W}] \right\} - \text{Tr} [\mathbf{W}^H \mathbf{C}_{1,w,k} \mathbf{W}] + \tilde{c}_{1,w,k}, \end{aligned} \quad (37)$$

where

$$\mathbf{B}_{1,w,k} \triangleq v_k u_{\text{U},k}^* \mathbf{t}_k \mathbf{h}_{\text{U},k}^H,$$

$$\mathbf{C}_{1,w,k} \triangleq v_k u_{\text{U},k}^* u_{\text{U},k} (1 + \kappa_{\text{r},k}) (\mathbf{h}_{\text{U},k} \mathbf{h}_{\text{U},k}^H + \kappa_t \text{diag}(\mathbf{h}_{\text{U},k} \mathbf{h}_{\text{U},k}^H)),$$

$$\tilde{c}_{1,w,k} \triangleq \log |v_k| - v_k u_{\text{U},k}^* u_{\text{U},k} \delta_{\text{U},k}^2 - v_k + 1.$$

Then, by using the identity $\text{Tr}[\mathbf{ABC}] = (\text{vec}(\mathbf{A}^T))^T (\mathbf{I} \otimes \mathbf{B}) \text{vec}(\mathbf{C})$ and $\text{Tr}[\mathbf{A}^T \mathbf{D}] = (\text{vec}(\mathbf{A}))^T \text{vec}(\mathbf{D})$ [35], we have

$$\tilde{f}_{1,k}(\tilde{\mathbf{w}}) = 2\text{Re} \left\{ \tilde{\mathbf{b}}_{1,w,k}^H \tilde{\mathbf{w}} \right\} - \tilde{\mathbf{w}}^H \tilde{\mathbf{C}}_{1,w,k} \tilde{\mathbf{w}} + \tilde{c}_{1,w,k}, \quad (38)$$

where

$$\tilde{\mathbf{b}}_{1,w,k} \triangleq \text{vec}(\mathbf{B}_{1,w,k}^H),$$

$$\tilde{\mathbf{C}}_{1,w,k} \triangleq \mathbf{I}_K \otimes \mathbf{C}_{1,w,k}.$$

2) *Mathematical Derivation of $\tilde{f}_{2,k}(\tilde{\mathbf{w}})$.* By using the identity $\text{Tr}[\mathbf{ABCD}] = (\text{vec}(\mathbf{D}^T))^T (\mathbf{C}^T \otimes \mathbf{A}) \text{vec}(\mathbf{B})$ [35], $\tilde{f}_{2,k}(\tilde{\mathbf{w}})$ in (23) can be reformulated as

$$\begin{aligned} \tilde{f}_{2,k}(\tilde{\mathbf{w}}) &= -\frac{d_k}{\delta_{E,k}^2} \left(\text{Tr} [\mathbf{h}_E \mathbf{h}_E^H \mathbf{W} \mathbf{t}_k \mathbf{t}_k^H \mathbf{W}^H] \right. \\ &\quad \left. + \kappa_t \text{Tr} [\mathbf{W}^H \text{diag}(\mathbf{h}_E \mathbf{h}_E^H) \mathbf{W}] \right) + \log d_k + 1 - d_k \\ &= -\frac{d_k}{\delta_{E,k}^2} \left(\tilde{\mathbf{w}}^H \left((\mathbf{t}_k \mathbf{t}_k^H)^T \otimes (\mathbf{h}_E \mathbf{h}_E^H) \right) \tilde{\mathbf{w}} \right. \\ &\quad \left. + \kappa_t \tilde{\mathbf{w}}^H (\mathbf{I}_K \otimes \text{diag}(\mathbf{h}_E \mathbf{h}_E^H)) \tilde{\mathbf{w}} \right) + \log d_k + 1 - d_k \\ &= -\tilde{\mathbf{w}}^H \tilde{\mathbf{C}}_{2,w,k} \tilde{\mathbf{w}} + \tilde{c}_{2,w,k}, \end{aligned} \quad (39)$$

where

$$\tilde{\mathbf{C}}_{2,w,k} \triangleq \frac{d_k}{\delta_{E,k}^2} \left((\mathbf{t}_k \mathbf{t}_k^H)^T \otimes (\mathbf{h}_E \mathbf{h}_E^H) \right) + \kappa_t (\mathbf{I}_K \otimes \text{diag}(\mathbf{h}_E \mathbf{h}_E^H)),$$

$$\tilde{c}_{2,w,k} \triangleq \log d_k + 1 - d_k.$$

Substituting (26), (38) and (39) into (36), the subproblem for $\tilde{\mathbf{w}}$ can be transformed into the following equivalent problem

$$\max_{\tilde{\mathbf{w}}} \min_{k \in \mathcal{K}} \left\{ \tilde{r}_k(\tilde{\mathbf{w}}) \right\} \quad (40a)$$

$$\text{s.t. } \tilde{\mathbf{w}}^H \tilde{\mathbf{w}} \leq P, \quad (40b)$$

where

$$\tilde{r}_k(\tilde{\mathbf{w}}) = \omega_k \tilde{R}_k(\tilde{\mathbf{w}}), \quad (41)$$

$$\tilde{R}_k(\tilde{\mathbf{w}}) = -\tilde{\mathbf{w}}^H \tilde{\mathbf{C}}_{w,k} \tilde{\mathbf{w}} + 2\text{Re} \left\{ \tilde{\mathbf{b}}_{w,k}^H \tilde{\mathbf{w}} \right\} + \tilde{c}_{w,k}, \quad (42)$$

and $\tilde{\mathbf{C}}_{w,k}$, $\tilde{\mathbf{b}}_{w,k}$ and $\tilde{c}_{w,k}$ are defined, respectively, as follows

$$\tilde{\mathbf{C}}_{w,k} \triangleq \tilde{\mathbf{C}}_{1,w,k} + \tilde{\mathbf{C}}_{2,w,k} + \tilde{\mathbf{C}}_{3,w},$$

$$\tilde{\mathbf{b}}_{w,k} \triangleq \tilde{\mathbf{b}}_{1,w,k} + \tilde{\mathbf{b}}_{3,w},$$

$$\tilde{c}_{w,k} \triangleq \tilde{c}_{1,w,k} + \tilde{c}_{2,w,k} + \tilde{c}_{3,w}.$$

Finally, by introducing the auxiliary variable δ_w , the optimization problem in (40) can be reformulated as

$$\max_{\tilde{\mathbf{w}}, \delta_w} \delta_w \quad (43a)$$

$$\text{s.t. } \tilde{r}_k(\tilde{\mathbf{w}}) \geq \delta_w, \forall k \in \mathcal{K}, \quad (43b)$$

$$\tilde{\mathbf{w}}^H \tilde{\mathbf{w}} \leq P. \quad (43c)$$

The obtained reformulation in (43) is an SOCP problem whose globally optimum solution $\tilde{\mathbf{w}}$ can be obtained by using

standard numerical optimization methods, such as CVX.

C. Optimization of the Reflection Coefficient Vector ϕ

In this subsection, ϕ is optimized under the assumption that all the other variables are kept fixed.

The lower bound $\tilde{f}_{3,\phi}$ in (30) is a quadratic function in the optimization variable. Therefore, we rewrite $\tilde{f}_{1,k}(\phi)$ and $\tilde{f}_{2,k}(\phi)$ as quadratic functions.

1) *Mathematical Derivation of $\tilde{f}_{1,k}(\phi)$.* By using the matrix identity in [35, Eq. (1.10.6)], $\tilde{f}_{1,k}(\phi)$ in (17) can be reformulated as

$$\begin{aligned} \tilde{f}_{1,k}(\phi) &= 2\text{Re} \left\{ v_k u_{\text{U},k}^* \text{Tr} \left[\mathbf{H}_{\text{BI}} \mathbf{w}_k \mathbf{h}_{\text{I},k}^{\text{H}} \Phi \right] \right\} \\ &\quad - \text{Tr} \left[v_k u_{\text{U},k}^* u_{\text{U},k} (1 + \kappa_{\text{r},k}) \mathbf{h}_{\text{I},k} \mathbf{h}_{\text{I},k}^{\text{H}} \Phi \mathbf{H}_{\text{BI}} \left(\mathbf{W} \mathbf{W}^{\text{H}} \right. \right. \\ &\quad \left. \left. + \kappa_{\text{t}} \text{diag} \left(\mathbf{W} \mathbf{W}^{\text{H}} \right) \right) \mathbf{H}_{\text{BI}}^{\text{H}} \Phi^{\text{H}} \right] + \log |v_k| \\ &\quad - v_k u_{\text{U},k}^* u_{\text{U},k} \delta_{\text{U},k}^2 - v_k + 1 \\ &= 2\text{Re} \left\{ \tilde{\mathbf{b}}_{1,\phi,k}^{\text{H}} \phi \right\} - \text{Tr} \left[\Phi^{\text{H}} \mathbf{h}_{\text{I},k} \mathbf{h}_{\text{I},k}^{\text{H}} \Phi \mathbf{C}_{1,\phi,k} \right] + \tilde{c}_{1,\phi,k} \\ &= 2\text{Re} \left\{ \tilde{\mathbf{b}}_{1,\phi,k}^{\text{H}} \phi \right\} - \phi^{\text{H}} \left((\mathbf{h}_{\text{I},k} \mathbf{h}_{\text{I},k}^{\text{H}}) \odot \mathbf{C}_{1,\phi,k}^{\text{T}} \right) \phi + \tilde{c}_{1,\phi,k} \\ &= 2\text{Re} \left\{ \tilde{\mathbf{b}}_{1,\phi,k}^{\text{H}} \phi \right\} - \phi^{\text{H}} \tilde{\mathbf{C}}_{1,\phi,k} \phi + \tilde{c}_{1,\phi,k}, \end{aligned} \quad (44)$$

where

$$\begin{aligned} \mathbf{C}_{1,\phi,k} &\triangleq v_k u_{\text{U},k}^* u_{\text{U},k} (1 + \kappa_{\text{r},k}) \mathbf{H}_{\text{BI}} \left(\mathbf{W} \mathbf{W}^{\text{H}} + \kappa_{\text{t}} \text{diag} \mathbf{W} \mathbf{W}^{\text{H}} \right) \mathbf{H}_{\text{BI}}^{\text{H}}, \\ \tilde{\mathbf{C}}_{1,\phi,k} &\triangleq (\mathbf{h}_{\text{I},k} \mathbf{h}_{\text{I},k}^{\text{H}}) \odot \mathbf{C}_{1,\phi,k}^{\text{T}}, \\ \tilde{\mathbf{b}}_{1,\phi,k} &\triangleq \left[v_k u_{\text{U},k}^* \mathbf{H}_{\text{BI}} \mathbf{w}_k \mathbf{h}_{\text{I},k}^{\text{H}} \right]_{1,1}, \dots, \left[v_k u_{\text{U},k}^* \mathbf{H}_{\text{BI}} \mathbf{w}_k \mathbf{h}_{\text{I},k}^{\text{H}} \right]_{M,M}^{\text{T}}, \\ \tilde{c}_{1,\phi,k} &\triangleq \log |v_k| - v_k u_{\text{U},k}^* u_{\text{U},k} \delta_{\text{U},k}^2 - v_k + 1. \end{aligned}$$

2) *Mathematical Derivation of $\tilde{f}_{2,k}(\phi)$.* Similarly, $\tilde{f}_{2,k}(\phi)$ in (23) can be reformulated as

$$\begin{aligned} \tilde{f}_{2,k}(\phi) &= -\frac{d_k}{\delta_{\text{E},k}^2} \left(\text{Tr} \left[\Phi^{\text{H}} \mathbf{g}_{\text{I}} \mathbf{g}_{\text{I}}^{\text{H}} \Phi \mathbf{H}_{\text{BI}} \left(\mathbf{w}_k \mathbf{w}_k^{\text{H}} \right. \right. \right. \\ &\quad \left. \left. \left. + \kappa_{\text{t}} \text{diag} \mathbf{W} \mathbf{W}^{\text{H}} \right) \mathbf{H}_{\text{BI}}^{\text{H}} \right] \right) + \log d_k + 1 - d_k \\ &= -\frac{d_k}{\delta_{\text{E},k}^2} \phi^{\text{H}} \left((\mathbf{g}_{\text{I}} \mathbf{g}_{\text{I}}^{\text{H}}) \odot \mathbf{C}_{2,\phi,k}^{\text{T}} \right) \phi + \log d_k + 1 - d_k \\ &= -\phi^{\text{H}} \tilde{\mathbf{C}}_{2,\phi,k} \phi + \tilde{c}_{2,\phi,k}, \end{aligned} \quad (45)$$

where

$$\begin{aligned} \mathbf{C}_{2,\phi,k} &\triangleq \mathbf{H}_{\text{BI}} \left(\mathbf{w}_k \mathbf{w}_k^{\text{H}} + \kappa_{\text{t}} \text{diag} \mathbf{W} \mathbf{W}^{\text{H}} \right) \mathbf{H}_{\text{BI}}^{\text{H}}, \\ \tilde{\mathbf{C}}_{2,\phi,k} &\triangleq \frac{d_k}{\delta_{\text{E}}^2} \left((\mathbf{g}_{\text{I}} \mathbf{g}_{\text{I}}^{\text{H}}) \odot \mathbf{C}_{2,\phi,k}^{\text{T}} \right), \\ \tilde{c}_{2,\phi,k} &\triangleq \log d_k + 1 - d_k. \end{aligned}$$

By substituting (30), (44) and (45) into (36), the optimization subproblem for ϕ is equivalent to

$$\max_{\phi} \min_{k \in \mathcal{K}} \{ \tilde{r}_k(\phi) \} \quad (46a)$$

$$\text{s.t. } \phi \in \mathcal{S}, \quad (46b)$$

where

$$\tilde{r}_k(\phi) = \omega_k \tilde{R}_k(\phi), \quad (47)$$

$$\tilde{R}_k(\phi) = -\phi^{\text{H}} \tilde{\mathbf{C}}_{\phi,k} \phi + 2\text{Re} \left\{ \tilde{\mathbf{b}}_{\phi,k}^{\text{H}} \phi \right\} + \tilde{c}_{\phi,k}, \quad (48)$$

Algorithm 1 BCD-SOCP Algorithm

Initialize: Initialize $\tilde{\mathbf{w}}^0$, ϕ^0 to feasible values and set $n=0$

- 1: **while** The value of the objective function in (36) has not converged **do**
- 2: Given $\tilde{\mathbf{w}}^n$ and ϕ^n , calculate \mathcal{U}^{n+1} , \mathcal{V}^{n+1} , \mathcal{D}^{n+1} , \mathcal{P}^{n+1} and \mathcal{Q}^{n+1} by using (19), (20), (24), (28), (32), (29) and (33);
- 3: Calculate $\tilde{\mathbf{w}}^{n+1}$ as the solution of the problem in (43) while ϕ^n , \mathcal{U}^{n+1} , \mathcal{V}^{n+1} , \mathcal{D}^{n+1} , \mathcal{P}^{n+1} and \mathcal{Q}^{n+1} are kept fixed;
- 4: Calculate ϕ^{n+1} as the solution of the problem in (49) while $\tilde{\mathbf{w}}^{n+1}$, \mathcal{U}^{n+1} , \mathcal{V}^{n+1} , \mathcal{D}^{n+1} , \mathcal{P}^{n+1} and \mathcal{Q}^{n+1} are kept fixed;
- 5: Set $n \leftarrow n + 1$
- 6: **end while**

and $\tilde{\mathbf{C}}_{\phi,k}$, $\tilde{\mathbf{b}}_{\phi,k}$ and $\tilde{c}_{\phi,k}$ are, respectively, given by

$$\begin{aligned} \tilde{\mathbf{C}}_{\phi,k} &\triangleq \tilde{\mathbf{C}}_{1,\phi,k} + \tilde{\mathbf{C}}_{2,\phi,k} + \tilde{\mathbf{C}}_{3,\phi}, \\ \tilde{\mathbf{b}}_{\phi,k} &\triangleq \tilde{\mathbf{b}}_{1,\phi,k}^* + \tilde{\mathbf{b}}_{3,\phi}^*, \\ \tilde{c}_{\phi,k} &\triangleq \tilde{c}_{1,\phi,k} + \tilde{c}_{2,\phi,k} + \tilde{c}_{3,\phi}. \end{aligned}$$

By introducing the auxiliary variable δ_{ϕ} , the problem in (46) can be rewritten as

$$\max_{\phi, \delta_{\phi}} \delta_{\phi} \quad (49a)$$

$$\text{s.t. } \tilde{r}_k(\phi) \geq \delta_{\phi}, \forall k \in \mathcal{K}, \quad (49b)$$

$$\phi \in \mathcal{S}. \quad (49c)$$

Due to the non-convex unit-modulus constraints in (49c), the problem in (49) is still non-convex. To tackle this issue, the SDR optimization method is used to relax it [36]. Specifically, we introduce the variables $\hat{\phi} = \begin{bmatrix} \phi \\ \phi_{M+1} \end{bmatrix}$ and $\Theta = \hat{\phi} \hat{\phi}^{\text{H}}$, and the latter matrix satisfies the conditions $\Theta \succeq 0$ and $\text{rank}(\Theta) = 1$. Accordingly, the problem (49) is transformed to

$$\max_{\Theta, \delta_{\phi}} \delta_{\phi} \quad (50a)$$

$$\text{s.t. } \hat{r}_k(\Theta) \geq \delta_{\phi}, \forall k \in \mathcal{K}, \quad (50b)$$

$$\Theta \succeq 0, \quad (50c)$$

$$\Theta_{m,m} = 1, m = 1, 2, \dots, M+1, \quad (50d)$$

where

$$\hat{r}_k(\Theta) = \omega_k \hat{R}_k(\Theta), \quad (51)$$

$$\hat{R}_k(\Theta) = -\text{Tr} \left[\hat{\mathbf{C}}_{\phi,k} \Theta \right] + \tilde{c}_{\phi,k}, \quad (52)$$

and

$$\hat{\mathbf{C}}_{\phi,k} \triangleq \begin{bmatrix} \tilde{\mathbf{C}}_{\phi,k} & -\tilde{\mathbf{b}}_{\phi,k} \\ -\tilde{\mathbf{b}}_{\phi,k}^{\text{H}} & 0 \end{bmatrix}. \quad (53)$$

The problem in (50) is an SOCP optimization problem, which can be solved by using conventional numerical optimization tools, such as CVX. Nevertheless, the optimal solution Θ for the problem (50) is not guaranteed to fulfill the constraint $\text{rank}(\Theta) = 1$. Thus, we adopt the Gaussian randomization approach [36] to obtain a rank-1 solution for ϕ at each iteration.

D. Algorithm Development

1) *BCD-SOCP Algorithm*: In Algorithm 1, we present the complete BCD-SOCP algorithm. Specifically, we maximize the WMSR by alternately optimizing the variables \mathcal{U} , \mathcal{V} , \mathcal{D} , \mathcal{P} , \mathcal{Q} , $\tilde{\mathbf{w}}$ and ϕ .

2) *Complexity Analysis*: The complexity of optimizing the auxiliary variables \mathcal{U} , \mathcal{V} , \mathcal{D} , \mathcal{P} and \mathcal{Q} is discussed first. The complexity order for computing each u_k in (19), v_k in (20), d_k in (24), and \mathcal{P} in (28) and (32), is given by $\mathcal{O}(K(M^2 + MN))$. Hence, the computation of \mathcal{U} , \mathcal{V} , \mathcal{D} , and \mathcal{P} has the same complexity order equal to $\mathcal{O}(K^2(M^2 + MN))$. Since the Cholesky decomposition and the Kronecker product applied to compute \mathbf{q}_w in (29) and \mathbf{q}_ϕ in (33), the overall complexity for computing \mathcal{Q} is $\mathcal{O}(N^3K^3/3 + N^2K^2 + M^2 + MN)$. Thus, the total computational complexity for obtaining \mathcal{U} , \mathcal{V} , \mathcal{D} , \mathcal{P} and \mathcal{Q} is $\mathcal{O}(N^3K^3/3 + N^2K^2 + M^2K^2 + MNK^2)$.

The computational complexity of calculating the main optimization variables corresponds to the complexity of solving the SOCP problems formulated in (43) and (50). According to [37], since the problem in (43) includes a power constraint and K rate constraints whose dimension is NK , the corresponding complexity is $\mathcal{O}(N^3K^{5.5})$. Similarly, the relaxed version of the problem in (50) includes $2K$ rate constraints of dimension M and M constant modulus constraints of dimension one. Thus, the corresponding complexity is $\mathcal{O}(M^{3.5} + M^3K^{2.5} + N^3K^{5.5})$.

In summary, the computational complexity of each iteration of Algorithm 1 is $\mathcal{O}(M^{3.5} + M^3K^{2.5} + N^3K^{5.5})$.

IV. BCD-MM ALGORITHM

In Algorithm 1, the use of CVX to solve the SOCP problems results in a large computational complexity, since high complexity optimization algorithms, such as the interior point method, are utilized. To reduce the computational complexity, we introduce, a BCD-MM algorithm. Specifically, since the objective functions in (40) and (46) are non-differentiable, we first derive smooth lower bound functions, and then apply the MM algorithm by introducing surrogate objective functions for the obtained lower bounds. We show that this approach results in a simple closed-form solution.

A. Approximate Functions

Based on [38], we approximate the objective functions in problems (40) and (46) as

$$\min_{k \in \mathcal{K}} \{\tilde{r}_k(\tilde{\mathbf{w}})\} \approx f(\tilde{\mathbf{w}}) = -\frac{1}{\zeta} \log \left(\sum_{k=1}^K \exp\{-\zeta \tilde{r}_k(\tilde{\mathbf{w}})\} \right), \quad (54)$$

$$\min_{k \in \mathcal{K}} \{\tilde{r}_k(\phi)\} \approx f(\phi) = -\frac{1}{\zeta} \log \left(\sum_{k=1}^K \exp\{-\zeta \tilde{r}_k(\phi)\} \right), \quad (55)$$

where $f(\tilde{\mathbf{w}})$ and $f(\phi)$ are lower bounds for the objective functions in (40) and (46), respectively, and $\zeta > 0$ is a smoothing parameter that satisfies the conditions:

$$f(\tilde{\mathbf{w}}) + \frac{1}{\zeta} \log(K) \geq \min_{k \in \mathcal{K}} \{\tilde{r}_k(\tilde{\mathbf{w}})\} \geq f(\tilde{\mathbf{w}}) \quad (56)$$

$$f(\phi) + \frac{1}{\zeta} \log(K) \geq \min_{k \in \mathcal{K}} \{\tilde{r}_k(\phi)\} \geq f(\phi). \quad (57)$$

In [39], the authors proved that $-\frac{1}{\mu} \log \left(\sum_{x \in \mathcal{X}} \exp\{-\mu x\} \right)$ is a concave function of x and is monotonically increasing. Additionally, $\tilde{r}_k(\tilde{\mathbf{w}})$ is a quadratic concave function of $\tilde{\mathbf{w}}$, and hence $f(\tilde{\mathbf{w}})$ is a concave function of $\tilde{\mathbf{w}}$. Similarly, $f(\phi)$ is a concave function of ϕ . The smoothing parameter ζ is optimized as described in [6]. Specifically, we set ζ equal to a small initial value, and then gradually increases it, to improve the approximation accuracy, until it reaches an upper limit ζ_{\max} . The advantage of this strategy is that it avoids local minima in the early stages of operation and avoids the loss of accuracy caused by the use of a large smoothing factor, which can degrade the performance of the MM algorithm.

B. Majorization-Minimization Method

Armed with the approximated functions in (54) and (55), we adopt the MM algorithm [40]. The MM algorithm does not directly optimize the functions in (54) and (55), but it operates on surrogate functions that are easier to optimize. Specifically, let us consider the maximization of the complex function $f(\mathbf{x})$ where \mathbf{x} belongs to a set \mathcal{S}_x . Let us consider the surrogate function $\tilde{f}(\mathbf{x}|\mathbf{x}^n)$ with given \mathbf{x}^n , where \mathbf{x}^n is the optimal solution that corresponds to the surrogate function at the $(n-1)$ -th iteration. The surrogate function $\tilde{f}(\mathbf{x}|\mathbf{x}^n)$ is said to minorize $f(\mathbf{x})$ at the given point \mathbf{x}^n if the following conditions are satisfied [40]

$$(A1) : \tilde{f}(\mathbf{x}^n|\mathbf{x}^n) = f(\mathbf{x}^n), \forall \mathbf{x}^n \in \mathcal{S}_x;$$

$$(A2) : \tilde{f}(\mathbf{x}|\mathbf{x}^n) \leq f(\mathbf{x}), \forall \mathbf{x}, \mathbf{x}^n \in \mathcal{S}_x;$$

$$(A3) : \tilde{f}'(\mathbf{x}^n|\mathbf{x}^n; \eta)|_{\mathbf{x}=\mathbf{x}^n} = f'(\mathbf{x}^n; \eta), \forall \eta \text{ with } \mathbf{x}^n + \eta \in \mathcal{S}_x;$$

$$(A4) : \tilde{f}(\mathbf{x}|\mathbf{x}^n) \text{ is continuous in } \mathbf{x} \text{ and } \mathbf{x}^n,$$

where $f'(\mathbf{x}^n; \eta)$ is the directional derivative of $f(\mathbf{x}^n)$, which is defined as

$$f'(\mathbf{x}^n; \eta) = \lim_{\lambda \rightarrow 0} \frac{f(\mathbf{x}^n + \lambda \eta) - f(\mathbf{x}^n)}{\lambda}. \quad (58)$$

A drawback of the MM algorithm is that it may need many iterations to converge. To circumvent this issue, the SQUAREM method [41] is used to accelerate the convergence of the MM algorithm and hence to reduce the computational overhead.

C. Optimization of the Precoding Vector $\tilde{\mathbf{w}}$

With $f(\tilde{\mathbf{w}})$ defined in (54), the subproblem in (40) can be transformed to the following problem

$$\max_{\tilde{\mathbf{w}}} f(\tilde{\mathbf{w}}) \quad (59a)$$

$$\text{s.t. } \tilde{\mathbf{w}}^H \tilde{\mathbf{w}} \leq P. \quad (59b)$$

A surrogate function for $f(\tilde{\mathbf{w}})$ is given in the following lemma.

Lemma 5: Let $\tilde{\mathbf{w}}^n$ be the solution at the $(n-1)$ -th iteration. For any feasible $\tilde{\mathbf{w}}$, $f(\tilde{\mathbf{w}})$ is minorized by the following quadratic function

$$\tilde{f}(\tilde{\mathbf{w}}|\tilde{\mathbf{w}}^n) = \bar{c}_w + 2\text{Re}\{\bar{\mathbf{v}}_w^H \tilde{\mathbf{w}}\} + \bar{\alpha} \tilde{\mathbf{w}}^H \tilde{\mathbf{w}}, \quad (60)$$

where

$$\bar{\mathbf{v}}_w \triangleq \sum_{k=1}^K h_{\tilde{\mathbf{w}},k}(\tilde{\mathbf{w}}^n) \left(\tilde{\mathbf{b}}_{w,k} - \tilde{\mathbf{C}}_{w,k}^H \tilde{\mathbf{w}}^n \right) - \bar{\alpha} \tilde{\mathbf{w}}^n, \quad (61a)$$

$$\bar{c}_w \triangleq f(\tilde{\mathbf{w}}^n) + \bar{\alpha} \tilde{\mathbf{w}}^{n,H} \tilde{\mathbf{w}}^n$$

$$-2\text{Re} \left\{ \sum_{k=1}^K h_{\tilde{\mathbf{w}},k}(\tilde{\mathbf{w}}^n) \left(\tilde{\mathbf{b}}_{w,k}^H - \tilde{\mathbf{w}}^{n,H} \tilde{\mathbf{C}}_{w,k} \right) \tilde{\mathbf{w}}^n \right\}, \quad (61b)$$

$$\bar{\alpha} \triangleq -\max_k \left\{ \text{Tr} \left[\tilde{\mathbf{C}}_{w,k} \right] \right\} - 2\zeta \max_k \left\{ \bar{o}_{w,k} \right\}, \quad (61c)$$

and $h_{\tilde{\mathbf{w}},k}(\tilde{\mathbf{w}}^n)$ and $\bar{o}_{w,k}$ are, respectively, given by

$$h_{\tilde{\mathbf{w}},k}(\tilde{\mathbf{w}}^n) \triangleq \frac{\exp \{-\zeta \tilde{r}_k(\tilde{\mathbf{w}}^n)\}}{\sum_{k=1}^K \exp \{-\zeta \tilde{r}_k(\tilde{\mathbf{w}}^n)\}}, \quad (62a)$$

$$\bar{o}_{w,k} \triangleq P \text{Tr} \left[\tilde{\mathbf{C}}_{w,k} \tilde{\mathbf{C}}_{w,k}^H \right] + \left\| \tilde{\mathbf{b}}_{w,k} \right\|_2^2 + 2\sqrt{P} \left\| \tilde{\mathbf{C}}_{w,k} \tilde{\mathbf{b}}_{w,k} \right\|_2. \quad (62b)$$

Proof: See Appendix C. ■

Therefore, the problem in (59) can be approximated as

$$\max_{\tilde{\mathbf{w}}} \bar{c}_w + 2\text{Re} \left\{ \bar{\mathbf{v}}_w^H \tilde{\mathbf{w}} \right\} + \bar{\alpha} \tilde{\mathbf{w}}^H \tilde{\mathbf{w}}, \quad (63a)$$

$$\text{s.t.} \quad \tilde{\mathbf{w}}^H \tilde{\mathbf{w}} \leq P. \quad (63b)$$

The optimization problem in (63) can be solved by using the method of Lagrangian multipliers. Specifically, the Lagrangian function is given by

$$L(\tilde{\mathbf{w}}, \varepsilon) = \bar{c}_w + 2\text{Re} \left\{ \bar{\mathbf{v}}_w^H \tilde{\mathbf{w}} \right\} + \bar{\alpha} \tilde{\mathbf{w}}^H \tilde{\mathbf{w}} - \varepsilon (\tilde{\mathbf{w}}^H \tilde{\mathbf{w}} - P), \quad (64)$$

where ε is the Lagrange multiplier. Therefore, the optimal solution $\tilde{\mathbf{w}}$ of the surrogate optimization problem in (64) at the n -th iteration is

$$\tilde{\mathbf{w}}^{n+1} = -\sqrt{\frac{P}{\bar{\mathbf{v}}_w^H \bar{\mathbf{v}}_w}} \bar{\mathbf{v}}_w. \quad (65)$$

D. Optimization of the Reflection Coefficient Vector ϕ

With $f(\phi)$ defined in (55), the subproblem in (46) can be transformed to the following problem

$$\max_{\phi} f(\phi) \quad (66a)$$

$$\text{s.t.} \quad \phi \in S. \quad (66b)$$

A surrogate function for $f(\phi)$ is given in the following lemma.

Lemma 6: Let ϕ^n be the solution at the $(n-1)$ -th iteration. For any feasible ϕ , $f(\phi)$ is minorized by the following function

$$\bar{f}(\phi|\phi^n) = 2\text{Re} \left\{ \bar{\mathbf{v}}_{\phi}^H \phi \right\} + \bar{c}_{\phi}, \quad (67)$$

where n is the iteration number, and

$$\bar{\mathbf{v}}_{\phi} \triangleq \sum_{k=1}^K h_{\phi,k}(\phi^n) \left(\tilde{\mathbf{b}}_{\phi,k} - \tilde{\mathbf{C}}_{\phi,k}^H \phi^n \right) - \bar{\beta} \phi^n, \quad (68a)$$

$$\bar{c}_{\phi} \triangleq \bar{f}(\phi^n) + 2M\bar{\beta} - 2\text{Re} \left\{ \sum_{k=1}^K h_{\phi,k}(\phi^n) \left(\tilde{\mathbf{b}}_{\phi,k}^H - \phi^{n,H} \tilde{\mathbf{C}}_{\phi,k} \right) \phi^n \right\}, \quad (68b)$$

with

$$h_{\phi,k}(\phi^n) \triangleq \frac{\exp \{-\zeta \tilde{r}_k(\phi^n)\}}{\sum_{k=1}^K \exp \{-\zeta \tilde{r}_k(\phi^n)\}}, \quad (69a)$$

$$\bar{\beta} \triangleq -\max_k \left\{ \lambda_{\max} \left(\tilde{\mathbf{C}}_{\phi,k} \right) \right\} \quad (69b)$$

$$-2\zeta \max_k \left\{ \left\| \tilde{\mathbf{b}}_{\phi,k} \right\|_2^2 + M\lambda_{\max} \left(\tilde{\mathbf{C}}_{\phi,k} \tilde{\mathbf{C}}_{\phi,k}^H \right) + 2 \left\| \tilde{\mathbf{C}}_{\phi,k} \tilde{\mathbf{b}}_{\phi,k} \right\|_1 \right\}.$$

Proof: See Appendix D. ■

Algorithm 2 BCD-MM algorithm

Initialize: Initialize $\tilde{\mathbf{w}}^0$, ϕ^0 to feasible values. Set $n = 0$, the smoothing factor ζ , the maximum value of the smoothing factor ζ_{\max} , the adjustment factor ι , the maximum number of iterations n_{\max} and the error tolerance ε .

- 1: **while** $|\mathcal{R}(\tilde{\mathbf{w}}^{n+1}, \phi^{n+1}) - \mathcal{R}(\tilde{\mathbf{w}}^n, \phi^n)| / \mathcal{R}(\tilde{\mathbf{w}}^n, \phi^n) \geq \varepsilon$ and $n \leq n_{\max}$ **do**
 - 2: Given $\tilde{\mathbf{w}}^n$ and ϕ^n , calculate \mathcal{U}^{n+1} , \mathcal{V}^{n+1} , \mathcal{D}^{n+1} , \mathcal{P}^{n+1} and \mathcal{Q}^{n+1} by using (19), (20), (24), (28), (32), (29) and (33);
 - 3: Calculate $\tilde{\mathbf{w}}_1 = \mathcal{F}_{\mathbf{W}}(\tilde{\mathbf{w}}^n)$ and $\tilde{\mathbf{w}}_2 = \mathcal{F}_{\mathbf{W}}(\tilde{\mathbf{w}}_1)$;
 - 4: Calculate $\mathbf{j}_1 = \tilde{\mathbf{w}}_1 - \tilde{\mathbf{w}}^n$ and $\mathbf{j}_2 = \tilde{\mathbf{w}}_2 - \tilde{\mathbf{w}}_1 - \mathbf{j}_1$;
 - 5: Calculate the step factor $\alpha = -\frac{\|\mathbf{j}_1\|_2}{\|\mathbf{j}_2\|_2}$;
 - 6: Calculate $\tilde{\mathbf{w}}^{n+1} = \tilde{\mathbf{w}}^n - 2\alpha\mathbf{j}_1 + \alpha^2\mathbf{j}_2$;
 - 7: If $\|\tilde{\mathbf{w}}^{n+1}\|_2 > \sqrt{P}$, set $\tilde{\mathbf{w}}^{n+1} \leftarrow \frac{\sqrt{P}}{\|\tilde{\mathbf{w}}^{n+1}\|_2} \tilde{\mathbf{w}}^{n+1}$;
 - 8: If $f(\tilde{\mathbf{w}}^{n+1}) < f(\tilde{\mathbf{w}}_2)$, set $\alpha \leftarrow \frac{(\alpha-1)}{2}$, back to step 4;
 - 9: Calculate $\phi_1 = \mathcal{F}_{\phi}(\phi^n)$ and $\phi_2 = \mathcal{F}_{\phi}(\phi_1)$;
 - 10: Calculate $\mathbf{k}_1 = \phi_1 - \phi^n$ and $\mathbf{k}_2 = \phi_2 - \phi_1 - \mathbf{k}_1$;
 - 11: Calculate the step factor $\beta = -\frac{\|\mathbf{k}_1\|_2}{\|\mathbf{k}_2\|_2}$;
 - 12: Calculate $\phi^{n+1} = \exp \left\{ \angle \left(\phi^n - 2\beta\mathbf{k}_1 + \beta^2\mathbf{k}_2 \right) \right\}$;
 - 13: If $f(\phi^{n+1}) < f(\phi_2)$, set $\beta \leftarrow \frac{(\beta-1)}{2}$, back to step 10;
 - 14: Set $\zeta \leftarrow \min(\zeta^{\iota}, \zeta_{\max})$ and $n \leftarrow n + 1$;
 - 15: **end while**
-

Therefore, the problem in (66) can be approximated as

$$\max_{\phi} 2\text{Re} \left\{ \bar{\mathbf{v}}_{\phi}^H \phi \right\} + \bar{c}_{\phi} \quad (70a)$$

$$\text{s.t.} \quad \phi \in S. \quad (70b)$$

The optimal solution ϕ^{n+1} at the n -th iteration is given by

$$\phi^{n+1} = \exp \{j\angle \bar{\mathbf{v}}_{\phi}\}, \quad (71)$$

where $\exp(\cdot)$ and $\angle(\cdot)$ are intended as element-wise functions.

E. Algorithm Development

1) *BCD-MM Algorithm:* The complete BCD-MM algorithm is summarized in Algorithm 2. Specifically, the optimization problems in (40) and (46) are transformed into the optimization problems in (63) and (70), whose approximate optimal solutions are given in (65) and (71), respectively. In Algorithm 2, the following notation is used: $\mathcal{R}(\cdot)$ is the objective function of the problem in (10); $\mathcal{F}_{\mathbf{W}}(\cdot)$ and $\mathcal{F}_{\phi}(\cdot)$ are the iteration updates for $\tilde{\mathbf{w}}$ and ϕ given in (65) and (71), respectively. In Step 14, the adjustment factor ι is used to successively increase the smoothness factor ζ from its initial value to ζ_{\max} .

2) *Complexity Analysis:* The computational complexity of optimizing the variables \mathcal{U} , \mathcal{V} , \mathcal{D} , \mathcal{P} and \mathcal{Q} is the same as in Section III-D, which is $\mathcal{O}(N^3K^3/3 + N^2K^2 + M^2K^2 + MNK^2)$. Next, we analyze the computational complexity of the two remaining optimization variables. Note that $r_{\tilde{\mathbf{w}},k}(\tilde{\mathbf{w}}^n)$ and $r_{\phi,k}(\tilde{\mathbf{w}}^n)$ can be reused when calculating $h_{\tilde{\mathbf{w}},k}(\tilde{\mathbf{w}}^n)$

and $h_{\phi,k}(\tilde{\mathbf{w}}^n)$, respectively. First, we note that the complexity required to calculate $h_{\tilde{\mathbf{w}},k}(\tilde{\mathbf{w}}^n)$ and $h_{\phi,k}(\tilde{\mathbf{w}}^n)$ is $\mathcal{O}(K(N^3K^3/3 + N^2K^2 + M^2 + MN))$ and $\mathcal{O}(KM^3)$, respectively.

As far the optimization of $\tilde{\mathbf{w}}$ is concerned, the complexity of computing $o_{\tilde{\mathbf{w}},k}$ and $\bar{\alpha}$ is $\mathcal{O}(N^2K^2)$ and $\mathcal{O}(K(N^2K^2))$, respectively. The complexity of calculating $\tilde{\mathbf{v}}_{\tilde{\mathbf{w}}}$ mainly depends on $h_{\tilde{\mathbf{w}},k}(\tilde{\mathbf{w}}^n)$. Hence, the complexity of computing $\tilde{\mathbf{w}}^{n+1}$ is $\mathcal{O}(K(N^3K^3/3 + N^2K^2 + M^2 + MN))$. As far as the computational complexity of the subproblems corresponding to ϕ is concerned, the complexity of computing $\lambda_{\max}(\tilde{\mathbf{C}}_{\phi,k}\tilde{\mathbf{C}}_{\phi,k}^H)$ is $\mathcal{O}(M^3)$ and the computational complexity required to find $\tilde{\beta}$ is $\mathcal{O}(KM^3)$. Hence, the complexity of calculating ϕ^{n+1} is $\mathcal{O}(KM^3)$.

Finally, the overall complexity of Algorithm 2 is $\mathcal{O}(M^2K + MNK + N^3K^4/3 + N^2K^3) + \mathcal{O}(M^3K)$. Therefore, the complexity of Algorithm 2 is lower than that of Algorithm 1.

V. SIMULATION RESULTS

A. Simulation Setup

In this section, simulation results are illustrated to evaluate the performance of the proposed BCD-SOCP and BCD-MM algorithms. Figure 2 depicts the considered simulation setup, wherein the BS and the RIS are located at (0 m, 0 m, 30 m) and $(x_{RIS}, 0 \text{ m}, 10 \text{ m})$, respectively. Unless stated otherwise, $x_{RIS} = 150 \text{ m}$. Three legitimate users are randomly located in a $20 \text{ m} \times 20 \text{ m}$ area, whose center is $(x_U, y_U, 1.5 \text{ m})$, and the eavesdropper is located at $(x_E, y_E, 1.5 \text{ m})$. We assume that $x_U = x_E = 150 \text{ m}$ and $y_U = y_E = 10 \text{ m}$. In addition, unless stated otherwise, the number of BS transmit antennas and RIS reflecting elements is $N = 4$ and $M = 16$, respectively.

The large-scale path loss is defined as

$$PL = -30 - 10\alpha \log_{10} d, \quad (72)$$

where α is the path loss exponent and d is the link distance in meters. The path loss exponents of the BS-RIS channel, RIS-user channel and RIS-eavesdropper channel are equal to $\alpha_{BR} = 2.2$, $\alpha_{RU} = 2.2$ and $\alpha_{RE} = 3.6$, respectively.

The small scale fading is assumed to obey a Rician distribution, and, therefore, the channel is

$$\tilde{\mathbf{H}} = \sqrt{\frac{\kappa}{\kappa + 1}} \tilde{\mathbf{H}}^{\text{LoS}} + \sqrt{\frac{1}{\kappa + 1}} \tilde{\mathbf{H}}^{\text{NLoS}}, \quad (73)$$

where κ is the Rician factor, $\tilde{\mathbf{H}}^{\text{LoS}}$ and $\tilde{\mathbf{H}}^{\text{NLoS}}$ denote the line-of-sight (LoS) and the non-line-of-sight (NLoS) components, respectively. $\tilde{\mathbf{H}}^{\text{LoS}}$ is defined as the product of the steering vectors of the transmitter and receiver, while $\tilde{\mathbf{H}}^{\text{NLoS}}$ is randomly generated according to a Rayleigh distribution with unit power. Unless stated otherwise, we set $\kappa = 3$.

The MOSEK solver [42] in the CVX toolbox is used to solve the SOCP problem in Algorithm 1. The final results are obtained by averaging over 200 independent channels. Unless stated otherwise, the simulation parameters are set as follows: the HI factors are $\kappa_t = \kappa_{r,k} = 0.1$, the BS transmit power is $P = 1 \text{ W}$, the channel bandwidth is 10 MHz, the weighting factors are $\omega_k = 1, \forall k$, the noise power density is -174 dBm/Hz, the

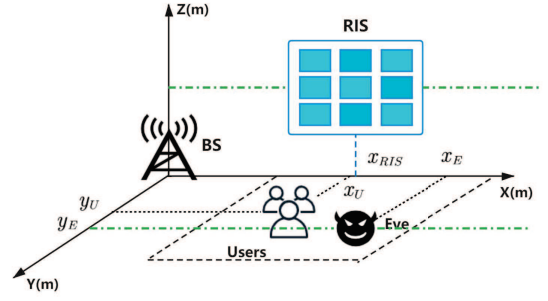
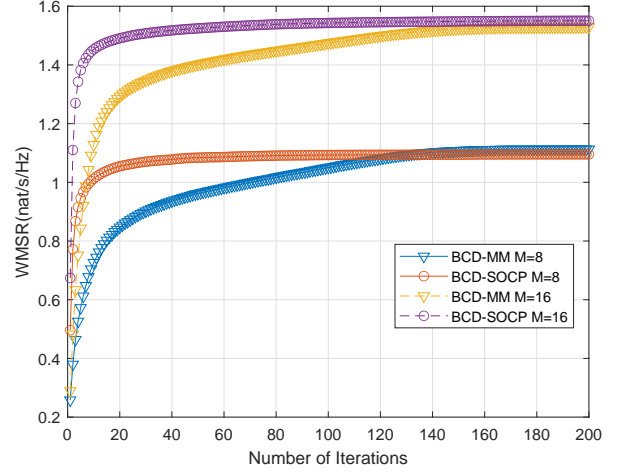
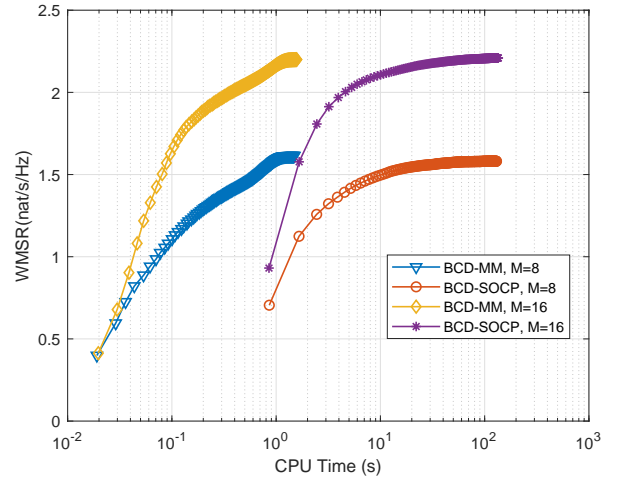


Fig. 2. The simulated RIS-assisted MISO communication scenario.



(a) Achievable WMSR versus the number of iterations



(b) Achievable WMSR versus the CPU time

Fig. 3. Convergence behavior of the proposed algorithms for $M = [8, 16]$

initial smoothing parameter is $\zeta = 1.25$, the adjustment factor is $\iota = 1.02$, the upper limit of the smoothing parameter is $\zeta_{\max} = 500$, and the error tolerance is $\varepsilon = 10^{-5}$.

B. Baseline Schemes

We compare the performance of the proposed algorithms with the following baseline schemes.

- 1) To verify the effectiveness of the proposed robust design, we implement a **Non-Robust** version of the proposed

approach that ignores the presence of HIs by setting $\kappa_t = \kappa_{r,k} = 0$ in Algorithm 2.

- 2) To study the advantages of jointly optimizing the precoding at the BS and the phase shifts at the RIS, we consider two case studies. The first algorithm optimizes only the precoding vector $\tilde{\mathbf{w}}$ and randomly selects ϕ . The corresponding algorithm is referred to as **BCD-MM-Rand**. The second algorithm uses maximum ratio transmission (MRT) [43] as the precoding vector of the BS and optimizes ϕ . The corresponding algorithm is referred to as **BCD-MM-MRT**.
- 3) In practice, it may be difficult and expensive to implement RISs that can adjust the phase shifts to any arbitrary continuous value. Therefore, we study the performance of Algorithm 2 when the phase shifts of the RIS are quantized with two bits, i.e., only four phase shifts can be realized. The corresponding scheme is referred to as **BCD-MM-2bit**. Specifically, let ϕ_m^{con} be the optimal phase shift of the m -th element of the RIS, which is obtained by applying the **BCD-MM** algorithm. Then, the corresponding 2-bit quantized phase shift is

$$\phi_m^{dis} = \exp \left\{ \arg \min_{\theta} |\angle \phi_m^{con} - \theta| \right\}, \quad (74)$$

where $\theta \in \{0, \frac{\pi}{2}, \pi, \frac{3\pi}{2}\}$.

C. Convergence Behavior of the Proposed Algorithms

Figure 3 illustrates the convergence behavior of the two proposed algorithms as a function of the number of RIS elements M . We see that the **BCD-MM** algorithm converges within 160 iterations, while the **BCD-SOCP** algorithm converges within 40 iterations. Compared with the **BCD-SOCP** algorithm, the **BCD-MM** algorithm converges to a similar value of the WMSR, but it requires less CPU time, which confirms the superiority of the **BCD-MM** algorithm. In addition, the obtained results show that the **BCD-MM** algorithm converges in almost the same number of iterations and CPU time for different values of M . This is mainly because the convergence speed of the MM algorithm is closely related to the approximation accuracy of the surrogate function, which is affected by the strategy for updating the smoothing factor.

D. Impact of the HIs Factor

The impact of the HIs factor is shown in Figure 4. We see that the security performance of the **Non-Robust** and **BCD-MM** algorithms degrades as the HIs factor increases. However, as the HI factor increases, the WMSR of the **BCD-MM** algorithm always outperforms the **Non-Robust** algorithm, which demonstrates the strength of the proposed robust transmission design. In addition, we see that the security performance of the **BCD-MM-Rand** and **BCD-MM-MRT** algorithms is always worse than that of the **BCD-MM** algorithm, which highlights the superiority of the joint optimization strategy. Since the **BCD-MM-Rand** algorithm does not attempt to optimize the phase shifts of the RIS, it offers the worst security performance. This substantiates the benefits of deploying an RIS for improving the secrecy rate.

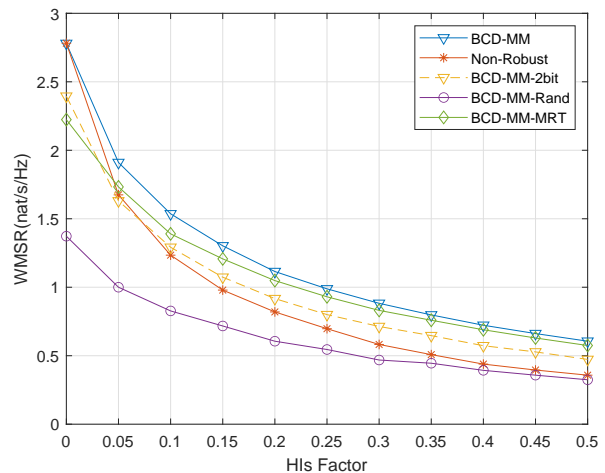


Fig. 4. Achievable WMSR versus the HIs factor

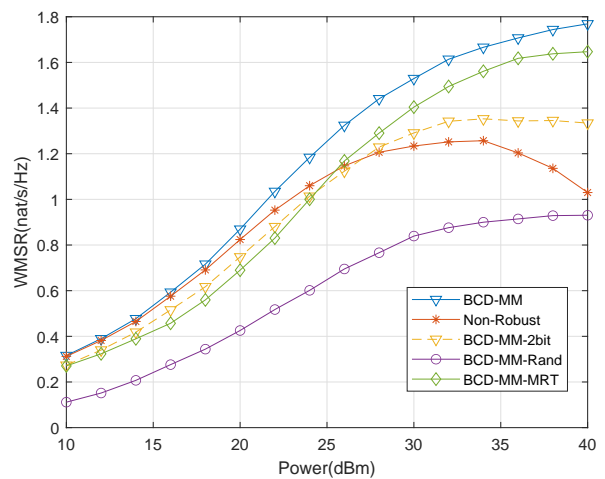


Fig. 5. Achievable WMSR versus the maximum transmit power

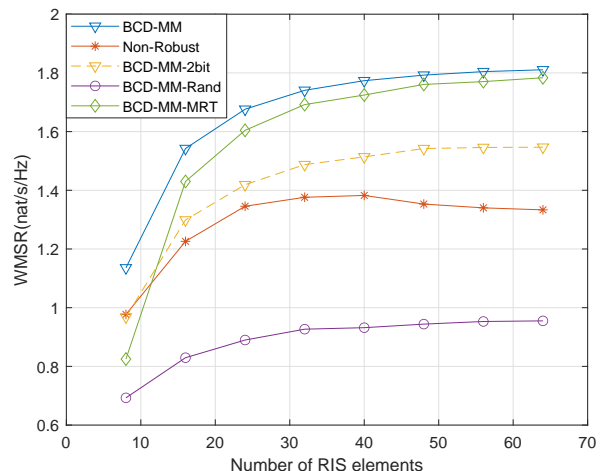


Fig. 6. Achievable WMSR versus the number of RIS elements M

E. Impact of the Maximum Transmit Power

Figure 5 illustrates the impact of the maximum transmit power on the WMSR. In this context, it is worth recalling that the distortion noise at the transceiver is assumed to be proportional to the signal power. Hence, increasing the signal power improves the SNR, but it increases the performance loss caused by the presence of HIs as well. We see that the security performance gap between the **Non-Robust** and the **BCD-MM** algorithms gradually increases as the transmit power increases. This is because the **Non-Robust** algorithm does not account for the HIs by design, and its performance degradation is more prominent. Additionally, we see that the WMSR of the **Non-Robust** algorithm gradually decreases when the transmit power is greater than 34 dBm, which further strengthen the necessity of designing robust algorithms in the high transmit power regime.

F. Impact of the Number of RIS Elements

Figure 6 illustrates the WMSR as a function of the number of RIS elements. As expected, increasing the number of RIS elements improves the secrecy rate. However, we clearly see a diminishing return law as a function of the RIS elements. In particular, only a marginal gain of the secrecy rate is observed when M increases from 40 to 64. In addition, the WMSR of the **Non-Robust** algorithm is significantly lower than that of the **BCD-MM-2bit** algorithm, which further corroborates the advantages of the proposed robust design against the HIs. Furthermore, the WMSR of the **BCD-MM-Rand** algorithm is much lower than that of the **BCD-MM-2bit** algorithm, which indicates the potential benefits of deploying an RIS for enhancing the secrecy rate.

VI. CONCLUSION

In this paper, we studied the secrecy rate of an RIS-aided multi-user wireless network in the presence of hardware impairments. We demonstrated that the deployment of an RIS can effectively increase the secrecy rate of the legitimate users through appropriate adjustment of the RIS phase shifts and the precoding matrix of the BS. We introduced a BCD framework for jointly optimizing the precoding at the BS and the phase shifts of the RIS. Specifically, we decoupled the original problem into two tractable subproblems and proposed an SOCP-based algorithm to alternately optimize them. To reduce the computational complexity, we proposed an MM algorithm based on surrogate functions that are formulated in a closed-form expression. Simulation results demonstrated the advantages of the proposed robust transmission design that accounts for the hardware impairments by design, as well the computational efficiency of the proposed solutions in terms of number of iterations and CPU time.

APPENDIX A PROOF OF LEMMA 3

By introducing the auxiliary variables p_w and \mathbf{q}_w , $f_3(\tilde{\mathbf{w}})$ in (14) can be written as

$$\begin{aligned}
f_3(\tilde{\mathbf{w}}) &= \log \left(1 + \frac{\mathbf{h}_E^H \Upsilon_t \mathbf{h}_E}{\delta_E^2} \right) \\
&= \log \left(1 + \frac{\kappa_t \text{Tr} [\mathbf{W}^H \text{diag} (\mathbf{h}_E \mathbf{h}_E^H) \mathbf{W}]}{\delta_E^2} \right) \\
&= \log \left(1 + \frac{\kappa_t \tilde{\mathbf{w}}^H (\mathbf{I}_K \otimes \text{diag} (\mathbf{h}_E \mathbf{h}_E^H)) \tilde{\mathbf{w}}}{\delta_E^2} \right) \\
&\stackrel{(b1)}{=} \log \left(1 + \frac{\tilde{\mathbf{w}}^H \mathbf{L}^T \mathbf{L} \tilde{\mathbf{w}}}{\delta_E^2} \right) \\
&= -\log \left(\frac{\delta_E^2}{|\mathbf{L} \tilde{\mathbf{w}}|^2 + \delta_E^2} \right) \\
&\stackrel{(a1)}{\geq} -p_w \left(\frac{\delta_E^2}{|\mathbf{L} \tilde{\mathbf{w}}|^2 + \delta_E^2} \right) + \log p_w + 1 \\
&\stackrel{(a2)}{\geq} -p_w \left((|\mathbf{L} \tilde{\mathbf{w}}|^2 + \delta_E^2) |\mathbf{q}_w|^2 - 2\text{Re} \{ \mathbf{q}_w^H \mathbf{L} \tilde{\mathbf{w}} \} + 1 \right) \\
&\quad + \log p_w + 1 \\
&= -\tilde{\mathbf{w}}^H \tilde{\mathbf{C}}_{3,w} \tilde{\mathbf{w}} + 2\text{Re} \{ \tilde{\mathbf{b}}_{3,w}^H \tilde{\mathbf{w}} \} + \tilde{c}_{3,w} = \tilde{f}_{3,\tilde{\mathbf{w}}}(\tilde{\mathbf{w}}),
\end{aligned}$$

where $\tilde{\mathbf{C}}_{3,w}$, $\tilde{\mathbf{b}}_{3,w}$ and $\tilde{c}_{3,w}$ are given in (27), and the Cholesky decomposition is applied in step (b1). Also, Lemma 1 and Lemma 2 are applied in steps (a1) and (a2), respectively. In step (a1), we set $\bar{x} = \frac{\delta_E^2}{|\mathbf{L} \tilde{\mathbf{w}}|^2 + \delta_E^2}$ and $\bar{y} = p_w$, and the optimal solution for p_w is given in (28). In step (a2), we set $\bar{\mathbf{x}} = \mathbf{L} \tilde{\mathbf{w}}$ and $\bar{\mathbf{y}} = \mathbf{q}_w$, and the optimal solution for \mathbf{q}_w is given in (29).

Hence, the proof is completed.

APPENDIX B PROOF OF LEMMA 4

Similar to Lemma 3, we introduce the auxiliary variables p_ϕ and \mathbf{q}_ϕ . Then, $f_3(\phi)$ in (14) can be formulated as

$$\begin{aligned}
f_3(\phi) &= \log \left(1 + \frac{\mathbf{h}_E^H \Upsilon_t \mathbf{h}_E}{\delta_E^2} \right) \\
&\stackrel{(b2)}{=} \log \left(1 + \frac{\mathbf{h}_E^H \mathbf{J}^T \mathbf{J} \mathbf{h}_E}{\delta_E^2} \right) \\
&= -\log \left(\frac{\delta_E^2}{|\mathbf{h}_E^H \mathbf{J}^T|^2 + \delta_E^2} \right) \\
&\stackrel{(a3)}{\geq} -p_\phi \left(\frac{\delta_E^2}{|\mathbf{h}_E^H \mathbf{J}^T|^2 + \delta_E^2} \right) + \log p_\phi + 1 \\
&\stackrel{(a4)}{\geq} -p_\phi \left((|\mathbf{h}_E^H \mathbf{J}^T|^2 + \delta_E^2) |\mathbf{q}_\phi|^2 - 2\text{Re} \{ \mathbf{h}_E^H \mathbf{J}^T \mathbf{q}_\phi \} + 1 \right) \\
&\quad + \log p_\phi + 1 \\
&= -p_\phi \left(\mathbf{g}_I^H \Phi \mathbf{H}_{\text{BI}} \mathbf{J}^T \mathbf{J} \mathbf{H}_{\text{BI}}^H \Phi^H \mathbf{g}_I + \delta_E^2 \right) |\mathbf{q}_\phi|^2 \\
&\quad + 2p_\phi \text{Re} \{ \mathbf{g}_I^H \Phi \mathbf{H}_{\text{BI}} \mathbf{J}^T \mathbf{q}_\phi \} - p_\phi + \log p_\phi + 1
\end{aligned}$$

$$\bar{\mathbf{N}}_w = -\sum_{k=1}^K \hat{g}_{\tilde{\mathbf{w}},k}(\eta) \left(\begin{bmatrix} \mathbf{I} \otimes \tilde{\mathbf{C}}_{\tilde{\mathbf{w}},k} & 0 \\ 0 & \mathbf{I} \otimes \tilde{\mathbf{C}}_{\tilde{\mathbf{w}},k}^H \end{bmatrix} + \mu \begin{bmatrix} \mathbf{e}_k \\ \mathbf{e}_k^* \end{bmatrix} \begin{bmatrix} \mathbf{e}_k \\ \mathbf{e}_k^* \end{bmatrix}^H \right) + \mu \begin{bmatrix} \sum_{k=1}^K \hat{g}_{\tilde{\mathbf{w}},k}(\eta) \mathbf{e}_k \\ \sum_{k=1}^K \hat{g}_{\tilde{\mathbf{w}},k}(\eta) \mathbf{e}_k^* \end{bmatrix} \begin{bmatrix} \sum_{k=1}^K \hat{g}_{\tilde{\mathbf{w}},k}(\eta) \mathbf{e}_k \\ \sum_{k=1}^K \hat{g}_{\tilde{\mathbf{w}},k}(\eta) \mathbf{e}_k^* \end{bmatrix}^H. \quad (89)$$

$$\begin{aligned}
&= -p_\phi |\mathbf{q}_\phi|^2 \text{Tr} \left[\Phi^H \mathbf{g}_I \mathbf{g}_I^H \Phi \mathbf{H}_{\text{BI}} \mathbf{J}^T \mathbf{J} \mathbf{H}_{\text{BI}}^H \right] \\
&\quad + 2p_\phi \text{Re} \left\{ \text{Tr} \left[\mathbf{H}_{\text{BI}} \mathbf{J}^T \mathbf{q}_\phi \mathbf{g}_I^H \Phi \right] \right\} \\
&\quad - p_\phi |\mathbf{q}_\phi|^2 \delta_E^2 - p_\phi + \log p_\phi + 1 \\
&= -p_\phi |\mathbf{q}_\phi|^2 \phi^H \left(\left(\mathbf{g}_I \mathbf{g}_I^H \right) \odot \left(\mathbf{H}_{\text{BI}} \mathbf{J}^T \mathbf{J} \mathbf{H}_{\text{BI}}^H \right)^T \right) \phi \\
&\quad + 2\text{Re} \left\{ \tilde{\mathbf{b}}_{3,\phi}^H \phi \right\} + \tilde{c}_{3,\phi} \\
&= -\phi^H \tilde{\mathbf{C}}_{3,\phi} \phi + 2\text{Re} \left\{ \tilde{\mathbf{b}}_{3,\phi}^H \phi \right\} + \tilde{c}_{3,\phi} = \tilde{f}_{3,\phi}(\phi),
\end{aligned}$$

where $\tilde{\mathbf{C}}_{3,\phi}$, $\tilde{\mathbf{b}}_{3,\phi}$ and $\tilde{c}_{3,\phi}$ are given in (27), and the Cholesky decomposition is applied in step (b2). Also, Lemma 1 and Lemma 2 are applied in steps (a3) and (a4), respectively. In step (a3), we set $\bar{x} = \frac{\delta_E^2}{|\mathbf{h}_E^H \mathbf{J}^T|^2 + \delta_E^2}$ and $\bar{y} = p_\phi$, and the optimal solution for p_ϕ is given in (32). In step (a4), we set $\bar{\mathbf{x}} = \mathbf{h}_E^H \mathbf{J}^T$ and $\bar{\mathbf{y}} = \mathbf{q}_\phi$, and the optimal solution for \mathbf{q}_ϕ is given in (33).

Hence, the proof is completed.

APPENDIX C PROOF OF LEMMA 5

Considering that the objective function $\tilde{r}_k(\tilde{\mathbf{w}})$ of the optimization problem in (40) is a quadratic function, we assume that there exists a minorizing function $\tilde{f}(\tilde{\mathbf{w}})$ satisfying the following quadratic form

$$\begin{aligned}
\tilde{f}(\tilde{\mathbf{w}}|\tilde{\mathbf{w}}^n) &= f(\tilde{\mathbf{w}}^n) + 2\text{Re} \left\{ \mathbf{g}_{\tilde{\mathbf{w}}}^H (\tilde{\mathbf{w}} - \tilde{\mathbf{w}}^n) \right\} \\
&\quad + (\tilde{\mathbf{w}} - \tilde{\mathbf{w}}^n)^H \mathbf{M}_{\tilde{\mathbf{w}}} (\tilde{\mathbf{w}} - \tilde{\mathbf{w}}^n), \quad (75)
\end{aligned}$$

where $\mathbf{g}_{\tilde{\mathbf{w}}} \in \mathbb{C}^{NK \times 1}$ and $\mathbf{M}_{\tilde{\mathbf{w}}} \in \mathbb{C}^{NK \times NK}$ are parameters to be determined. For $\tilde{f}(\tilde{\mathbf{w}})$ to be a minorizing function, it needs to fulfill the conditions (A1)-(A4).

To this end, we derive $\mathbf{g}_{\tilde{\mathbf{w}}}$ and $\mathbf{M}_{\tilde{\mathbf{w}}}$ that satisfy the conditions (A1) - (A4). By substituting $\tilde{\mathbf{w}}$ into $\tilde{f}(\tilde{\mathbf{w}}|\tilde{\mathbf{w}}^n)$, it can be verified that $\tilde{f}(\tilde{\mathbf{w}})$ satisfies condition (A1). Since $\tilde{f}(\tilde{\mathbf{w}})$ is a quadratic function, in addition, the condition (A4) is satisfied. Hence, $\mathbf{g}_{\tilde{\mathbf{w}}}$ and $\mathbf{M}_{\tilde{\mathbf{w}}}$ need to be determined in order to fulfill the conditions (A2) and (A3).

First, we derive an expression for $\mathbf{g}_{\tilde{\mathbf{w}}}$ that fulfills (A3), which requires that the first-order derivatives of $f(\tilde{\mathbf{w}}^n)$ and

$\tilde{f}(\tilde{\mathbf{w}}|\tilde{\mathbf{w}}^n)$ are equal in any direction. Let $\tilde{\mathbf{w}}^m$ belongs to $\mathcal{S}_{\tilde{\mathbf{w}}}$. The directional derivative of $f(\tilde{\mathbf{w}})$ in the direction $\tilde{\mathbf{w}}^m - \tilde{\mathbf{w}}^n$ is given by

$$2\text{Re} \left\{ \sum_{k=1}^K h_{\tilde{\mathbf{w}},k}(\tilde{\mathbf{w}}^n) \left(\tilde{\mathbf{b}}_{w,k}^H - (\tilde{\mathbf{w}}^n)^H \tilde{\mathbf{C}}_{w,k} \right) (\tilde{\mathbf{w}}^m - \tilde{\mathbf{w}}^n) \right\}, \quad (76)$$

where $h_{\tilde{\mathbf{w}},k}(\tilde{\mathbf{w}}^n)$ is defined in (62a). Moreover, the directional derivative of $\tilde{f}(\tilde{\mathbf{w}}|\tilde{\mathbf{w}}^n)$ in (75) evaluated at $\tilde{\mathbf{w}}^n$ in the same direction is given by

$$2\text{Re} \left\{ \mathbf{g}_{\tilde{\mathbf{w}}}^H (\tilde{\mathbf{w}}^m - \tilde{\mathbf{w}}^n) \right\}. \quad (77)$$

Therefore, the vector $\mathbf{g}_{\tilde{\mathbf{w}}}$ is derived as

$$\mathbf{g}_{\tilde{\mathbf{w}}} = \sum_{k=1}^K h_{\tilde{\mathbf{w}},k}(\tilde{\mathbf{w}}^n) \left(\tilde{\mathbf{b}}_{w,k} - \tilde{\mathbf{C}}_{w,k}^H \tilde{\mathbf{w}}^n \right). \quad (78)$$

Then, we derive an expression for $\mathbf{M}_{\tilde{\mathbf{w}}}$ that fulfills (A2). This requires that $\tilde{f}(\tilde{\mathbf{w}}|\tilde{\mathbf{w}}^n)$ is a lower bound of $f(\tilde{\mathbf{w}})$ for each linear cut in any direction. Therefore, for any auxiliary variable $\eta \in [0, 1]$ and $\tilde{\mathbf{w}}^m \in \mathcal{S}_{\tilde{\mathbf{w}}}$, $\mathbf{M}_{\tilde{\mathbf{w}}}$ needs to be chosen so that the following expression is fulfilled

$$\begin{aligned}
f(\tilde{\mathbf{w}}^n + \eta(\tilde{\mathbf{w}}^m - \tilde{\mathbf{w}}^n)) &\geq f(\tilde{\mathbf{w}}^n) \\
&\quad + 2\eta \text{Re} \left\{ \mathbf{g}_{\tilde{\mathbf{w}}}^H (\tilde{\mathbf{w}} - \tilde{\mathbf{w}}^n) \right\} \\
&\quad + \eta^2 (\tilde{\mathbf{w}} - \tilde{\mathbf{w}}^n)^H \mathbf{M}_{\tilde{\mathbf{w}}} (\tilde{\mathbf{w}} - \tilde{\mathbf{w}}^n). \quad (79)
\end{aligned}$$

Let us define $\bar{m}_{\tilde{\mathbf{w}}}(\eta) \triangleq f(\tilde{\mathbf{w}}^n + \eta(\tilde{\mathbf{w}}^m - \tilde{\mathbf{w}}^n))$ and $\bar{n}_{\tilde{\mathbf{w}}}(\eta) \triangleq f(\tilde{\mathbf{w}}^n) + \eta^2 (\tilde{\mathbf{w}}^m - \tilde{\mathbf{w}}^n)^H \mathbf{M}_{\tilde{\mathbf{w}}} (\tilde{\mathbf{w}}^m - \tilde{\mathbf{w}}^n) + 2\eta \text{Re} \left\{ \mathbf{g}_{\tilde{\mathbf{w}}}^H (\tilde{\mathbf{w}}^m - \tilde{\mathbf{w}}^n) \right\}$. By direct inspection, we note that $\bar{m}_{\tilde{\mathbf{w}}}(0)$ is equal to $\bar{n}_{\tilde{\mathbf{w}}}(0)$. Also, the first-order derivative of $\bar{m}_{\tilde{\mathbf{w}}}(\eta)$ is given by

$$\nabla_\eta \bar{m}_{\tilde{\mathbf{w}}}(\eta) = \sum_{k=1}^K \hat{g}_{w,k}(\eta) \nabla_\eta \hat{h}_{w,k}(\eta), \quad (80)$$

where

$$\hat{h}_{w,k}(\eta) \triangleq h_{w,k}(\tilde{\mathbf{w}}^n + \eta(\tilde{\mathbf{w}}^m - \tilde{\mathbf{w}}^n)), \quad (81a)$$

$$\hat{g}_{w,k}(\eta) \triangleq \frac{\exp \left\{ -\mu \hat{h}_{w,k}(\eta) \right\}}{\sum_{k=1}^K \exp \left\{ -\mu \hat{h}_{w,k}(\eta) \right\}}, \quad (81b)$$

$$\begin{aligned}
\bar{\alpha} &= \lambda_{\min}(\bar{\mathbf{N}}_{\tilde{\mathbf{w}}}) \stackrel{(a1)}{\geq} - \sum_{k=1}^K \tilde{g}_{w,k}(\eta) \left(\lambda_{\max} \left(\begin{bmatrix} \mathbf{I} \otimes \tilde{\mathbf{C}}_{w,k} & 0 \\ 0 & \mathbf{I} \otimes \tilde{\mathbf{C}}_{w,k}^H \end{bmatrix} \right) + \mu \lambda_{\max} \left(\begin{bmatrix} \mathbf{e}_k \\ \mathbf{e}_k^* \end{bmatrix} \begin{bmatrix} \mathbf{e}_k \\ \mathbf{e}_k^* \end{bmatrix}^H \right) \right) \\
&\quad + \mu \lambda_{\min} \left(\begin{bmatrix} \sum_{k=1}^K \tilde{g}_{w,k}(\eta) \mathbf{e}_k \\ \sum_{k=1}^K \tilde{g}_{w,k}(\eta) \mathbf{e}_k^* \end{bmatrix} \begin{bmatrix} \sum_{k=1}^K \tilde{g}_{w,k}(\eta) \mathbf{e}_k \\ \sum_{k=1}^K \tilde{g}_{w,k}(\eta) \mathbf{e}_k^* \end{bmatrix}^H \right) \\
&\stackrel{(a2)}{=} - \sum_{k=1}^K \tilde{g}_{w,k}(\eta) \left(\lambda_{\max}(\tilde{\mathbf{C}}_{w,k}) + 2\mu \mathbf{e}_k^H \mathbf{e}_k \right) \stackrel{(a3)}{\geq} - \max_k \left\{ \lambda_{\max}(\tilde{\mathbf{C}}_{w,k}) \right\} - 2\mu \max_k \left\{ \|\mathbf{e}_k\|_2^2 \right\}. \quad (93)
\end{aligned}$$

$$\begin{aligned}
\|\mathbf{e}_k\|_2^2 &= \left\| \tilde{\mathbf{b}}_{w,k} - \tilde{\mathbf{C}}_{w,k}^H (\tilde{\mathbf{w}}^n + \eta(\tilde{\mathbf{w}}^m - \tilde{\mathbf{w}}^n)) \right\|_2^2 \\
&= \left\| \tilde{\mathbf{b}}_{w,k} \right\|_2^2 + \left\| \tilde{\mathbf{C}}_{w,k}^H (\tilde{\mathbf{w}}^n + \eta(\tilde{\mathbf{w}}^m - \tilde{\mathbf{w}}^n)) \right\|_2^2 - 2\text{Re} \left\{ \tilde{\mathbf{b}}_{w,k}^H \tilde{\mathbf{C}}_{w,k}^H (\tilde{\mathbf{w}}^n + \eta(\tilde{\mathbf{w}}^m - \tilde{\mathbf{w}}^n)) \right\} \\
&\stackrel{(a4)}{\leq} \lambda_{\max}(\tilde{\mathbf{C}}_{w,k} \tilde{\mathbf{C}}_{w,k}^H) \|\tilde{\mathbf{w}}^n + \eta(\tilde{\mathbf{w}}^m - \tilde{\mathbf{w}}^n)\|_2^2 + \left\| \tilde{\mathbf{b}}_{w,k} \right\|_2^2 - 2\text{Re} \left\{ \tilde{\mathbf{b}}_{w,k}^H \tilde{\mathbf{C}}_{w,k}^H (\tilde{\mathbf{w}}^n + \eta(\tilde{\mathbf{w}}^m - \tilde{\mathbf{w}}^n)) \right\} \\
&\stackrel{(a5)}{\leq} P \lambda_{\max}(\tilde{\mathbf{C}}_{w,k} \tilde{\mathbf{C}}_{w,k}^H) + \left\| \tilde{\mathbf{b}}_{w,k} \right\|_2^2 + 2\sqrt{P} \left\| \tilde{\mathbf{C}}_{w,k} \tilde{\mathbf{b}}_{w,k} \right\|_2 \quad (94)
\end{aligned}$$

$$\begin{aligned} \nabla_{\eta} \hat{h}_{\tilde{\mathbf{w}},k}(\eta) &= -2\eta(\tilde{\mathbf{w}}^m - \tilde{\mathbf{w}}^n)^H \tilde{\mathbf{C}}_{\tilde{\mathbf{w}},k}(\tilde{\mathbf{w}}^m - \tilde{\mathbf{w}}^n) \\ &+ 2\text{Re}\left\{\tilde{\mathbf{b}}_{\tilde{\mathbf{w}},k}^H(\tilde{\mathbf{w}}^m - \tilde{\mathbf{w}}^n) - (\tilde{\mathbf{w}}^n)^H \tilde{\mathbf{C}}_{\tilde{\mathbf{w}},k}(\tilde{\mathbf{w}}^m - \tilde{\mathbf{w}}^n)\right\}. \end{aligned} \quad (81c)$$

It can be verified that $\nabla_{\eta} \bar{m}_{\tilde{\mathbf{w}}}(\eta)$ is equal to $\nabla_{\eta} \bar{n}_{\tilde{\mathbf{w}}}(\eta)$. Hence, we obtain the sufficient condition for (79) as follows

$$\nabla_{\eta}^2 \bar{m}_{\tilde{\mathbf{w}}}(\eta) \geq \nabla_{\eta}^2 \bar{n}_{\tilde{\mathbf{w}}}(\eta), \forall \eta \in [0, 1]. \quad (82)$$

Next, we further manipulate (82) to solve for $\mathbf{M}_{\tilde{\mathbf{w}}}$. To this end, we define

$$\mathbf{e}_k \triangleq \tilde{\mathbf{b}}_{\tilde{\mathbf{w}},k} - \tilde{\mathbf{C}}_{\tilde{\mathbf{w}},k}^H(\tilde{\mathbf{w}}^n + \eta(\tilde{\mathbf{w}}^m - \tilde{\mathbf{w}}^n)), \quad (83)$$

$$\bar{\mathbf{w}} \triangleq \tilde{\mathbf{w}}^m - \tilde{\mathbf{w}}^n, \quad (84)$$

so that $\nabla_{\eta}^2 \bar{n}_{\tilde{\mathbf{w}}}(\eta)$ can be derived as

$$\begin{aligned} \nabla_{\eta}^2 \bar{n}_{\tilde{\mathbf{w}}}(\eta) &= 2(\tilde{\mathbf{w}}^m - \tilde{\mathbf{w}}^n)^H \mathbf{M}_{\tilde{\mathbf{w}}}(\tilde{\mathbf{w}}^m - \tilde{\mathbf{w}}^n) \\ &= 2\bar{\mathbf{w}}^H (\mathbf{I} \otimes \mathbf{M}_{\tilde{\mathbf{w}}}) \bar{\mathbf{w}} \\ &= [\bar{\mathbf{w}}^H \quad \bar{\mathbf{w}}^T] \begin{bmatrix} \mathbf{I} \otimes \mathbf{M}_{\tilde{\mathbf{w}}} & 0 \\ 0 & \mathbf{I} \otimes \mathbf{M}_{\tilde{\mathbf{w}}}^T \end{bmatrix} \begin{bmatrix} \bar{\mathbf{w}} \\ \bar{\mathbf{w}}^* \end{bmatrix}, \end{aligned} \quad (85)$$

where we used $\text{Tr}(\mathbf{ABC}) = (\text{vec}(\mathbf{A}^T))^T (\mathbf{I} \otimes \mathbf{B}) \text{vec}(\mathbf{C})$ [35].

Similarly, $\nabla_{\eta}^2 \bar{m}_{\tilde{\mathbf{w}}}(\eta)$ is given by

$$\begin{aligned} \nabla_{\eta}^2 \bar{m}_{\tilde{\mathbf{w}}}(\eta) &= \sum_{k \in \mathcal{K}} \left(\hat{g}_{\tilde{\mathbf{w}},k}(\eta) \nabla_{\eta}^2 \hat{h}_{\tilde{\mathbf{w}},k}(\eta) - \mu \hat{g}_{\tilde{\mathbf{w}},k}(\eta) \left(\nabla_{\eta} \hat{h}_{\tilde{\mathbf{w}},k}(\eta) \right)^2 \right) \\ &+ \mu \left(\sum_{k \in \mathcal{K}} \hat{g}_{\tilde{\mathbf{w}},k}(\eta) \nabla_{\eta} \hat{h}_{\tilde{\mathbf{w}},k}(\eta) \right)^2 \\ &= [\bar{\mathbf{w}}^H \quad \bar{\mathbf{w}}^T] \bar{\mathbf{N}}_{\tilde{\mathbf{w}}} \begin{bmatrix} \bar{\mathbf{w}} \\ \bar{\mathbf{w}}^* \end{bmatrix}, \end{aligned} \quad (86)$$

where

$$\nabla_{\eta} \hat{h}_{\tilde{\mathbf{w}},k}(\eta) = 2\text{Re}\{\mathbf{e}_k^H \bar{\mathbf{w}}\}, \quad (87)$$

$$\nabla_{\eta}^2 \hat{h}_{\tilde{\mathbf{w}},k}(\eta) = -2\bar{\mathbf{w}}^H \tilde{\mathbf{C}}_{\tilde{\mathbf{w}},k} \bar{\mathbf{w}}, \quad (88)$$

and $\bar{\mathbf{N}}_{\tilde{\mathbf{w}}}$ is given in (89) at the bottom of the previous page.

As a result, we have

$$\bar{\mathbf{N}}_{\tilde{\mathbf{w}}} \succeq \begin{bmatrix} \mathbf{I} \otimes \mathbf{M}_{\tilde{\mathbf{w}}} & 0 \\ 0 & \mathbf{I} \otimes \mathbf{M}_{\tilde{\mathbf{w}}}^T \end{bmatrix}. \quad (90)$$

Choosing $\mathbf{M}_{\tilde{\mathbf{w}}} = \bar{\alpha} \mathbf{I} = \lambda_{\min}(\bar{\mathbf{N}}_{\tilde{\mathbf{w}}}) \mathbf{I}$, (75) can be rewritten as

$$\bar{f}(\tilde{\mathbf{w}}|\tilde{\mathbf{w}}^n) = \bar{c}_w + 2\text{Re}\{\bar{\mathbf{v}}_w^H \tilde{\mathbf{w}}\} + \bar{\alpha} \tilde{\mathbf{w}}^H \tilde{\mathbf{w}}, \quad (91)$$

where $\bar{\mathbf{v}}_w$ and \bar{c}_w are given in (61a) and (61b), respectively.

However, the complexity of computing $\bar{\alpha}$ cannot be ignored.

We introduce the following lemmas to reduce the complexity:

- (a1) $\lambda_{\min}(\mathbf{A}) + \lambda_{\min}(\mathbf{B}) \leq \lambda_{\min}(\mathbf{A} + \mathbf{B})$, if \mathbf{A} and \mathbf{B} are Hermitian matrices [44];
- (a2) $\lambda_{\max}(\mathbf{A}) = \text{Tr}(\mathbf{A})$ and $\lambda_{\min}(\mathbf{A}) = 0$, if \mathbf{A} is a rank one matrix [44];
- (a3) $\sum_{m=1}^M a_m b_m \leq \max_{m=1}^M \{b_m\}$, if $a_m, b_m \geq 0$ and $\sum_{m=1}^M a_m = 1$ [45, Theorem 30];
- (a4) $\text{Tr}(\mathbf{AB}) \leq \lambda_{\max}(\mathbf{A}) \text{Tr}(\mathbf{B})$, if \mathbf{A} and \mathbf{B} are positive semidefinite matrices [44].

Additionally, it can be readily verified that

$$(a5) \quad -\sqrt{P} \|\mathbf{Bc}\|_2 \text{ is the solution to the following problem:} \quad (92a)$$

$$\min_{\mathbf{x}} \quad \text{Re}\{\mathbf{c}^H \mathbf{B}^H \mathbf{x}\} \quad (92a)$$

$$\text{s.t.} \quad \mathbf{x}^H \mathbf{x} \leq P. \quad (92b)$$

Using the inequalities (a1) and (a3) and the equalities (a2), a lower bound for $\bar{\alpha}$ can be derived as given in (93) at the bottom of the previous page.

Recall that $\tilde{\mathbf{w}} = \tilde{\mathbf{w}}^n + \eta(\tilde{\mathbf{w}}^m - \tilde{\mathbf{w}}^n)$, $\forall \eta \in [0, 1]$, thus $\|\tilde{\mathbf{w}} - \tilde{\mathbf{w}}^n + \eta(\tilde{\mathbf{w}}^m - \tilde{\mathbf{w}}^n)\|_2 \leq \sqrt{P}$. Furthermore, using (a4) and (a5), an upper bound for $\|\mathbf{e}_k\|_2^2$ can be derived as given in (94) at the bottom of this page.

Finally, by combining (93) with (94), we obtain the simple lower bound for $\bar{\alpha}$ in (61c).

Hence, the proof is completed.

APPENDIX D PROOF OF LEMMA 6

Similar to the proof of Lemma 5, we first derive a quadratic function $f(\phi|\phi^n)$, which satisfies the conditions (A1) and (A4), to minorize $f(\phi)$ as follows

$$\begin{aligned} \bar{f}(\phi|\phi^n) &= f(\phi^n) + 2\text{Re}\{\mathbf{g}_{\phi}^H(\phi - \phi^n)\} \\ &+ (\phi - \phi^n)^H \mathbf{M}_{\phi}(\phi - \phi^n), \end{aligned} \quad (95)$$

where the parameters $\mathbf{M}_{\phi} \in \mathbb{C}^{M \times M}$ and $\mathbf{g}_{\phi} \in \mathbb{C}^{M \times 1}$ are determined by the conditions (A2) and (A3).

To satisfy the condition (A3), the directional derivatives of the left and right hand sides of (95) need to be equal in any direction, which yields

$$\mathbf{g}_{\phi} = \sum_{k=1}^K h_{\phi,k}(\phi^n) \left(\tilde{\mathbf{b}}_{\phi,k} - \tilde{\mathbf{C}}_{\phi,k}^H \phi^n \right), \quad (96)$$

where $h_{\phi,k}(\phi^n)$ is defined in (69a).

$$\bar{\mathbf{N}}_{\phi} = - \sum_{k=1}^K \tilde{g}_{\phi,k}(\eta) \left(\begin{bmatrix} \mathbf{I} \otimes \tilde{\mathbf{C}}_{\phi,k} & 0 \\ 0 & \mathbf{I} \otimes \tilde{\mathbf{C}}_{\phi,k}^H \end{bmatrix} + \zeta \begin{bmatrix} \mathbf{o}_k \\ \mathbf{o}_k^* \end{bmatrix} \begin{bmatrix} \mathbf{o}_k \\ \mathbf{o}_k^* \end{bmatrix}^H \right) + \zeta \begin{bmatrix} \sum_{k=1}^K \tilde{g}_{\phi,k}(\eta) \mathbf{o}_k \\ \sum_{k=1}^K \tilde{g}_{\phi,k}(\eta) \mathbf{o}_k^* \end{bmatrix} \begin{bmatrix} \sum_{k=1}^K \tilde{g}_{\phi,k}(\eta) \mathbf{o}_k \\ \sum_{k=1}^K \tilde{g}_{\phi,k}(\eta) \mathbf{o}_k^* \end{bmatrix}^H \quad (103)$$

$$\begin{aligned} \bar{\beta} &= \lambda_{\min}(\bar{\mathbf{N}}_{\phi}) \stackrel{(a1)}{\geq} - \sum_{k=1}^K \tilde{g}_{\phi,k}(\eta) \left(\lambda_{\max} \left(\begin{bmatrix} \mathbf{I} \otimes \tilde{\mathbf{C}}_{\phi,k} & 0 \\ 0 & \mathbf{I} \otimes \tilde{\mathbf{C}}_{\phi,k}^H \end{bmatrix} \right) + \zeta \lambda_{\max} \left(\begin{bmatrix} \mathbf{o}_k \\ \mathbf{o}_k^* \end{bmatrix} \begin{bmatrix} \mathbf{o}_k \\ \mathbf{o}_k^* \end{bmatrix}^H \right) \right) \\ &+ \zeta \lambda_{\min} \left(\begin{bmatrix} \sum_{k=1}^K \tilde{g}_{\phi,k}(\eta) \mathbf{o}_k \\ \sum_{k=1}^K \tilde{g}_{\phi,k}(\eta) \mathbf{o}_k^* \end{bmatrix} \begin{bmatrix} \sum_{k=1}^K \tilde{g}_{\phi,k}(\eta) \mathbf{o}_k \\ \sum_{k=1}^K \tilde{g}_{\phi,k}(\eta) \mathbf{o}_k^* \end{bmatrix}^H \right) \\ &\stackrel{(a2)}{=} - \sum_{k=1}^K \tilde{g}_{\phi,k}(\eta) \left(\lambda_{\max}(\tilde{\mathbf{C}}_{\phi,k}) + 2\zeta \mathbf{o}_k^H \mathbf{o}_k \right) \stackrel{(a3)}{\geq} - \max_k \left\{ \lambda_{\max}(\tilde{\mathbf{C}}_{\phi,k}) \right\} - 2\zeta \max_k \left\{ \|\mathbf{o}_k\|_2^2 \right\}. \end{aligned} \quad (106)$$

For condition (A2), we consider a relaxed condition (A2'), where the domain of ϕ is replaced with a relaxed feasible region $\mathcal{S}^{\text{relax}} \triangleq \{\phi \mid |\phi_m| \leq 1, 1 \leq m \leq M\}$. To satisfy condition (A2'), by defining $\phi = \phi^n + \eta(\phi^m - \phi^n)$, $\forall \eta \in [0, 1]$, we have

$$f(\phi^n + \eta(\phi^m - \phi^n)) \geq f(\phi^n) + 2\eta \text{Re} \{ \mathbf{g}_\phi^H (\phi^m - \phi^n) \} + \eta^2 (\phi - \phi^n)^H \mathbf{M}_\phi (\phi - \phi^n). \quad (97)$$

Similar to Appendix C, (98) is a sufficient condition for (97) to hold, i.e.,

$$\nabla_\eta^2 \bar{m}_\phi(\eta) \geq \nabla_\eta^2 \bar{n}_\phi(\eta), \forall \eta \in [0, 1], \quad (98)$$

where $\bar{m}_\phi(\eta)$ and $\bar{n}_\phi(\eta)$ represent the left and right hand sides of (97), respectively.

Then, to obtain the expression for \mathbf{M}_ϕ , we calculate the second-order derivatives of $\bar{m}_\phi(\eta)$ and $\bar{n}_\phi(\eta)$. We first define

$$\mathbf{o}_k \triangleq \tilde{\mathbf{b}}_{\phi,k} - \tilde{\mathbf{C}}_{\phi,k}^H (\phi^n + \eta(\phi^m - \phi^n)), \quad (99)$$

$$\bar{\phi} \triangleq \phi^m - \phi^n, \quad (100)$$

so that $\nabla_\eta^2 \bar{m}_\phi(\eta)$ can be written as

$$\nabla_\eta^2 \bar{m}_\phi(\eta) = [\bar{\phi}^H \quad \bar{\phi}^T] \bar{\mathbf{N}}_\phi \begin{bmatrix} \bar{\phi} \\ \bar{\phi}^* \end{bmatrix}, \quad (101)$$

where

$$\hat{h}_{\phi,k}(\eta) \triangleq \tilde{r}_k(\phi^n + \eta(\phi^m - \phi^n)), \quad (102a)$$

$$\hat{g}_{\phi,k}(\eta) \triangleq \frac{\exp\{-\zeta \tilde{r}_k(\phi^n)\}}{\sum_{k=1}^K \exp\{-\zeta \tilde{r}_k(\phi^n)\}}, \quad (102b)$$

and

$$\nabla_\eta \hat{h}_{\phi,k}(\eta) = 2\text{Re} \left\{ \tilde{\mathbf{b}}_{\phi,k} (\phi^m - \phi^n) - \phi^{n,H} \tilde{\mathbf{C}}_{\phi,k} (\phi^m - \phi^n) \right\} - 2\eta (\phi^m - \phi^n)^H \tilde{\mathbf{C}}_{\phi,k} (\phi^m - \phi^n), \quad (102c)$$

$$\begin{aligned} \nabla_\eta^2 \hat{h}_{\phi,k}(\eta) &= -2(\phi^m - \phi^n)^H \tilde{\mathbf{C}}_{\phi,k} (\phi^m - \phi^n) \\ &= -2\bar{\phi}^H (\mathbf{I} \otimes \tilde{\mathbf{C}}_{\phi,k}) \bar{\phi} \\ &= [\bar{\phi}^H \quad \bar{\phi}^T] \begin{bmatrix} \mathbf{I} \otimes \tilde{\mathbf{C}}_{\phi,k} & 0 \\ 0 & \mathbf{I} \otimes \tilde{\mathbf{C}}_{\phi,k}^H \end{bmatrix} \begin{bmatrix} \bar{\phi} \\ \bar{\phi}^* \end{bmatrix}, \end{aligned} \quad (102d)$$

and $\bar{\mathbf{N}}_\phi$ is defined in (103) at the bottom of the previous page.

In addition, $\nabla_\eta^2 \bar{n}_\phi(\eta)$ can be further rewritten as

$$\begin{aligned} \nabla_\eta^2 \bar{n}_\phi(\eta) &= 2(\phi - \phi^n)^H \mathbf{M}_\phi (\phi - \phi^n) \\ &= 2\bar{\phi}^H (\mathbf{I} \otimes \mathbf{M}_\phi) \bar{\phi} \\ &= [\bar{\phi}^H \quad \bar{\phi}^T] \begin{bmatrix} \mathbf{I} \otimes \mathbf{M}_\phi & 0 \\ 0 & \mathbf{I} \otimes \mathbf{M}_\phi^T \end{bmatrix} \begin{bmatrix} \bar{\phi} \\ \bar{\phi}^* \end{bmatrix}. \end{aligned} \quad (104)$$

As a result, we have

$$\bar{\mathbf{N}}_\phi \succeq \begin{bmatrix} \mathbf{I} \otimes \mathbf{M}_\phi & 0 \\ 0 & \mathbf{I} \otimes \mathbf{M}_\phi^T \end{bmatrix}. \quad (105)$$

For simplicity, we choose $\mathbf{M}_\phi = \bar{\beta} \mathbf{I} = \lambda_{\min}(\bar{\mathbf{N}}_\phi) \mathbf{I}$. By using the properties (a1)-(a3) in Appendix C, we replace $\bar{\beta}$ with its lower bound, as shown in (106) at the bottom of this page. From the unit-modulus constraints, we have $\phi^H \phi = (\phi^n)^H \phi^n = M$.

Then, we introduce the following result to deal with $\|\mathbf{o}_k\|_2^2$: (a6) $-\|\mathbf{B}\mathbf{c}\|_1$ is the solution to the following problem for $\mathbf{x} = [x_1, \dots, x_M]^T$:

$$\min_{\mathbf{x}} \text{Re} \{ \mathbf{c}^H \mathbf{B} \mathbf{H} \mathbf{x} \} \quad (107a)$$

$$\text{s.t. } |x_m| \leq 1, 1 \leq m \leq M. \quad (107b)$$

By using (a4) in Appendix C and (a6), we obtain the upper bound for $\|\mathbf{o}_k\|_2^2$ given in (108) at the bottom of this page. The lower bound of $\bar{\beta}$ is independent of η . Hence, the conclusion based on the condition (A2') satisfies the condition (A2) as well.

Finally, (95) can be rewritten as

$$\bar{f}(\phi|\phi^n) = 2\text{Re} \{ \bar{\mathbf{v}}_\phi^H \phi \} + \bar{c}_\phi, \quad (109)$$

where $\bar{\mathbf{v}}_\phi$ and \bar{c}_ϕ are given in (68a) and (68b), respectively.

Hence, the proof is completed.

REFERENCES

- [1] ITU-R, *IMT Vision - Framework and overall objectives of the future development of IMT for 2020 and beyond*, ITU Recommendation M. 2083, Sep. 2015.
- [2] F. Tariq, M. R. A. Khandaker, K.-K. Wong, M. A. Imran, M. Bennis, and M. Debbah, "A speculative study on 6G," *IEEE Wireless Commun.*, vol. 27, no. 4, pp. 118–125, Aug. 2020.
- [3] C. Pan, H. Ren, K. Wang, J. F. Kolb, M. ElKashlan, M. Chen, M. Di Renzo, Y. Hao, J. Wang, A. L. Swindlehurst, X. You, and L. Hanzo, "Reconfigurable intelligent surfaces for 6G systems: Principles, applications, and research directions," *IEEE Commun. Mag.*, vol. 59, no. 6, pp. 14–20, Jun. 2021.
- [4] W. Chen, X. Ma, Z. Li, and N. Kuang, "Sum-rate maximization for intelligent reflecting surface based terahertz communication systems," in *Proc. IEEE/CIC Int. Conf. Commun. Workshops China (ICCC Workshops)*, Aug. 2019, pp. 153–157.
- [5] C. Liaskos, S. Nie, A. Tsioliariidou, A. Pitsillides, S. Ioannidis, and I. Akyildiz, "A new wireless communication paradigm through software-controlled metasurfaces," *IEEE Commun. Mag.*, vol. 56, no. 9, pp. 162–169, 2018.
- [6] Z. Peng, Z. Zhang, C. Pan, L. Li, and A. L. Swindlehurst, "Multiuser full-duplex two-way communications via intelligent reflecting surface," *IEEE Trans. Signal Process.*, vol. 69, pp. 837–851, Jan. 2021.
- [7] Q. Wu, S. Zhang, B. Zheng, C. You, and R. Zhang, "Intelligent reflecting surface-aided wireless communications: A tutorial," *IEEE Trans. Commun.*, vol. 69, no. 5, pp. 3313–3351, May 2021.

$$\begin{aligned} \|\mathbf{o}_k\|_2^2 &= \left\| \tilde{\mathbf{b}}_{\phi,k} - \tilde{\mathbf{C}}_{\phi,k}^H (\phi^n + \eta(\phi^m - \phi^n)) \right\|_2^2 \\ &= \left\| \tilde{\mathbf{b}}_{\phi,k} \right\|_2^2 + \left\| \tilde{\mathbf{C}}_{\phi,k}^H (\phi^n + \eta(\phi^m - \phi^n)) \right\|_2^2 - 2\text{Re} \left\{ \tilde{\mathbf{b}}_{\phi,k}^H \tilde{\mathbf{C}}_{\phi,k}^H (\phi^n + \eta(\phi^m - \phi^n)) \right\} \\ &\stackrel{(a4)}{\leq} \lambda_{\max} \left(\tilde{\mathbf{C}}_{\phi,k} \tilde{\mathbf{C}}_{\phi,k}^H \right) \left\| \phi^n + \eta(\phi^m - \phi^n) \right\|_2^2 + \left\| \tilde{\mathbf{b}}_{\phi,k} \right\|_2^2 - 2\text{Re} \left\{ \tilde{\mathbf{b}}_{\phi,k}^H \tilde{\mathbf{C}}_{\phi,k}^H (\phi^n + \eta(\phi^m - \phi^n)) \right\} \\ &\stackrel{(a6)}{\leq} M \lambda_{\max} \left(\tilde{\mathbf{C}}_{\phi,k} \tilde{\mathbf{C}}_{\phi,k}^H \right) + \left\| \tilde{\mathbf{b}}_{\phi,k} \right\|_2^2 + 2 \left\| \tilde{\mathbf{C}}_{\phi,k} \tilde{\mathbf{b}}_{\phi,k} \right\|_1. \end{aligned} \quad (108)$$

- [8] M. Di Renzo, A. Zappone, M. Debbah, M.-S. Alouini, C. Yuen, J. de Rosny, and S. Tretyakov, "Smart radio environments empowered by reconfigurable intelligent surfaces: How it works, state of research, and the road ahead," *IEEE J. Sel. Areas Commun.*, vol. 38, no. 11, pp. 2450–2525, Nov. 2020.
- [9] B. Zheng, C. You, and R. Zhang, "Intelligent reflecting surface assisted multi-user OFDMA: Channel estimation and training design," *IEEE Trans. Wireless Commun.*, vol. 19, no. 12, pp. 8315–8329, Dec. 2020.
- [10] M. Di Renzo, K. Ntontin, J. Song, F. H. Danufane, X. Qian, F. Lazarakis, J. De Rosny, D.-T. Phan-Huy, O. Simeone, R. Zhang, M. Debbah, G. Lerosey, M. Fink, S. Tretyakov, and S. Shamai, "Reconfigurable intelligent surfaces vs. relaying: Differences, similarities, and performance comparison," *IEEE Open J. Commun. Soc.*, vol. 1, pp. 798–807, 2020.
- [11] M. Di Renzo, F. H. Danufane, and S. Tretyakov, "Communication models for reconfigurable intelligent surfaces: From surface electromagnetics to wireless networks optimization," 2021. [Online]. Available: <https://arxiv.org/abs/2110.00833>
- [12] Q. Wu and R. Zhang, "Intelligent reflecting surface enhanced wireless network via joint active and passive beamforming," *IEEE Trans. Wireless Commun.*, vol. 18, no. 11, pp. 5394–5409, Aug. 2019.
- [13] Q. Wu and R. Zhang, "Towards smart and reconfigurable environment: Intelligent reflecting surface aided wireless network," *IEEE Commun. Mag.*, vol. 58, no. 1, pp. 106–112, Jan. 2020.
- [14] X. Yu, D. Xu, and R. Schober, "Enabling secure wireless communications via intelligent reflecting surfaces," in *Proc. IEEE Global Commun. Conf. (GLOBECOM)*, Waikoloa, HI, USA, Dec. 2019.
- [15] J. Liu, J. Zhang, Q. Zhang, J. Wang, and X. Sun, "Secrecy rate analysis for reconfigurable intelligent surface-assisted MIMO communications with statistical CSI," *China Communications*, vol. 18, no. 3, pp. 52–62, Mar. 2021.
- [16] D. Xu, X. Yu, Y. Sun, D. W. K. Ng, and R. Schober, "Resource allocation for secure IRS-assisted multiuser MISO systems," in *Proc. IEEE Globecom Workshops (GC Wkshps)*, Waikoloa, HI, USA, Dec. 2019.
- [17] K. Cumanan, Z. Ding, B. Sharif, G. Y. Tian, and K. K. Leung, "Secrecy rate optimizations for a MIMO secrecy channel with a multiple-antenna eavesdropper," *IEEE Trans. Veh. Technol.*, vol. 63, no. 4, pp. 1678–1690, 2014.
- [18] A. Almohamad, A. M. Tahir, A. Al-Kababji, H. M. Furqan, T. Khattab, M. O. Hasna, and H. Arslan, "Smart and secure wireless communications via reflecting intelligent surfaces: A short survey," *IEEE Open J. Commun. Soc.*, vol. 1, pp. 1442–1456, 2020.
- [19] M. Cui, G. Zhang, and R. Zhang, "Secure wireless communication via intelligent reflecting surface," *IEEE Wireless Commun. Lett.*, vol. 8, no. 5, pp. 1410–1414, Oct. 2019.
- [20] L. Yang, J. Yang, W. Xie, M. O. Hasna, T. Tsiftsis, and M. Di Renzo, "Secrecy performance analysis of RIS-aided wireless communication systems," *IEEE Trans. Veh. Technol.*, vol. 69, no. 10, pp. 12 296–12 300, Oct 2020.
- [21] X. Yu, D. Xu, Y. Sun, D. W. K. Ng, and R. Schober, "Robust and secure wireless communications via intelligent reflecting surfaces," *IEEE J. Sel. Areas Commun.*, vol. 38, no. 11, pp. 2637–2652, 2020.
- [22] H. Yang, Z. Xiong, J. Zhao, D. Niyato, L. Xiao, and Q. Wu, "Deep reinforcement learning-based intelligent reflecting surface for secure wireless communications," *IEEE Trans. Wireless Commun.*, vol. 20, no. 1, pp. 375–388, Jan. 2021.
- [23] G. Sun, X. Tao, N. Li, and J. Xu, "Intelligent reflecting surface and UAV assisted secrecy communication in millimeter-wave networks," *IEEE Trans. Veh. Technol.*, pp. 1–1, 2021.
- [24] E. Björnson, J. Hoydis, M. Kountouris, and M. Debbah, "Massive MIMO systems with non-ideal hardware: Energy efficiency, estimation, and capacity limits," *IEEE Trans. Inf. Theory*, vol. 60, no. 11, pp. 7112–7139, 2014.
- [25] H. Shen, W. Xu, S. Gong, C. Zhao, and D. W. K. Ng, "Beamforming optimization for IRS-aided communications with transceiver hardware impairments," *IEEE Trans. Commun.*, vol. 69, no. 2, pp. 1214–1227, Oct. 2021.
- [26] G. Zhou, C. Pan, H. Ren, K. Wang, and Z. Peng, "Secure wireless communication in RIS-aided MISO system with hardware impairments," *IEEE Wireless Commun. Lett.*, vol. 10, no. 6, pp. 1309–1313, Mar. 2021.
- [27] Q. Chen, M. Li, X. Yang, R. Alturki, M. D. Alshehri, and F. Khan, "Impact of residual hardware impairment on the IoT secrecy performance of RIS-assisted noma networks," *IEEE Access*, vol. 9, pp. 42 583–42 592, Mar. 2021.
- [28] J. Zhu, D. W. K. Ng, N. Wang, R. Schober, and V. K. Bhargava, "Analysis and design of secure massive MIMO systems in the presence of hardware impairments," *IEEE Trans. Wireless Commun.*, vol. 16, no. 3, pp. 2001–2016, Jan. 2017.
- [29] Y. Liu, E. Liu, and R. Wang, "Energy efficiency analysis of intelligent reflecting surface system with hardware impairments," in *Proc. IEEE Global Communications Conference*, 2020.
- [30] J. Zhu, R. Schober, and V. K. Bhargava, "Secure transmission in multicell massive MIMO systems," *IEEE Trans. Wireless Commun.*, vol. 13, no. 9, pp. 4766–4781, Sep. 2014.
- [31] Q. Shi, M. Razaviyayn, Z.-Q. Luo, and C. He, "An iteratively weighted MMSE approach to distributed sum-utility maximization for a MIMO interfering broadcast channel," *IEEE Trans. Signal Process.*, vol. 59, no. 9, pp. 4331–4340, 2011.
- [32] C. Pan, H. Zhu, N. J. Gomes, and J. Wang, "Joint precoding and RRH selection for user-centric green MIMO C-RAN," *IEEE Trans. Wireless Commun.*, vol. 16, no. 5, pp. 2891–2906, May 2017.
- [33] X. Guan, Q. Wu, and R. Zhang, "Intelligent reflecting surface assisted secrecy communication: Is artificial noise helpful or not?" *IEEE Wireless Commun. Lett.*, vol. 9, no. 6, pp. 778–782, June 2020.
- [34] G. Zhou, C. Pan, H. Ren, K. Wang, K. K. Chai, and K.-K. Wong, "User cooperation for IRS-aided secure SWIPT MIMO systems," 2021. [Online]. Available: <https://arxiv.org/abs/2006.05347>
- [35] X. Zhang, *Matrix analysis and applications*. Beijing, CHN: Tsinghua University Press, 2004.
- [36] Q. Wu and R. Zhang, "Intelligent reflecting surface enhanced wireless network: Joint active and passive beamforming design," in *Proc. IEEE Global Commun. Conf. (GLOBECOM)*, Dec. 2018, pp. 1–6.
- [37] A. Ben-Tal and A. Nemirovski, *Lectures on modern convex optimization: Analysis, algorithms, and engineering applications*. Philadelphia, PA, USA: Society for Industrial and Applied Mathematics, 2001.
- [38] S. Xu, "Smoothing method for minimax problems," *Comput. Optim. Appl.*, vol. 20, no. 3, pp. 267–279, Dec. 2001.
- [39] G. Zhou, C. Pan, H. Ren, K. Wang, and A. Nallanathan, "Intelligent reflecting surface aided multigroup multicast MISO communication systems," *IEEE Trans. Signal Process.*, vol. 68, pp. 3236–3251, Apr. 2020.
- [40] Y. Sun, P. Babu, and D. P. Palomar, "Majorization-minimization algorithms in signal processing, communications, and machine learning," *IEEE Trans. Signal Process.*, vol. 65, no. 3, pp. 794–816, Feb. 2017.
- [41] R. Varadhan and C. Roland, "Simple and globally convergent methods for accelerating the convergence of any EM algorithm," *Scand. J. Stat.*, vol. 35, no. 2, pp. 335–353, Jun. 2008.
- [42] MOSEK-ApS, *The MOSEK optimization toolbox for MATLAB manual*, Version 9.2 (Revision 14), Jun. 2020.
- [43] Q. Wu and R. Zhang, "Beamforming optimization for wireless network aided by intelligent reflecting surface with discrete phase shifts," *IEEE Transactions on Communications*, vol. 68, no. 3, pp. 1838–1851, Mar. 2020.
- [44] H. Lütkepohl, *Handbook of matrices*. New York, NY, USA: Wiley, 1996.
- [45] J. R. Magnus and H. Neudecker, *Matrix differential calculus with applications in statistics and econometrics*. Hoboken, NJ, USA: Wiley, 1988.